Dynamical Solvent Effects on Activated Electron-Transfer Reactions: Principles, Pitfalls, and Progress†

MICHAEL J. WEAVER

Department of Chemistry, Purdue University, West Lafayette, Indiana 47907

Received July 30, 1991 (Revised Manuscript Received February 14, 1992)

Contents

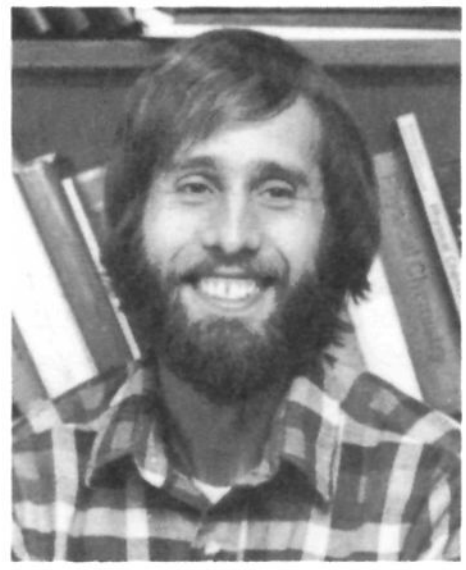

Michael J. Weaver was born in London, England, in 1947. Following doctoral research at Imperial College with Douglas Inman, he was a research fellow at Caltech under Fred Anson from 1972 to 1975. After a period on the faculty at Michigan State University, he moved to Purdue University in 1982 where he has been Professor of Chemistry since 1985. His current research interests span electrochemistry, electron-transfer chemistry, surface vibrational spectroscopies and scanning microscopies, and electrochemical surface science. He is continually amazed by (and grateful for) the diversity of research disciplines, and inspiring scientific colleagues, that a physical electrochemist can stumble upon.

I. Introduction

Understanding the various influences exerted by the solvating environment upon the kinetics of electron-transfer (ET) processes, either in homogeneous solution or at metal–solution and related interfaces, has long captured the attention of experimentalists and theoreticians alike. Traditionally, these roles have been perceived primarily in terms of *energetic* factors, whereby the solvent is considered to affect the reaction rates via its influence on the net activation barrier to electron transfer, ΔG^*. Indeed, such considerations form a mainstay of the well-known Marcus and related theoretical treatments.[1] In these approaches, solvent effects upon ΔG^* are separated into so-called intrinsic and extrinsic (or thermodynamic) factors. The latter encompasses the various solvent influences upon ΔG^* attributed to the reaction free energy, $\Delta G°$, whereas the former describes the barrier component present in the absence of this driving force.

The physical origin of the intrinsic solvent (or "outer-shell") barrier, ΔG^*_{os}, is in the need for the reorganization of surrounding solvent dipoles to occur to some extent prior to the (essentially instantaneous) electron-transfer act itself. Description of ΔG^*_{os} in terms of the conventional dielectric-continuum model leads to well-known expressions, based on a nonequilibrium "Born-charging" treatments, that contain the so-called Pekar factor ($\epsilon_{op}^{-1} - \epsilon_0^{-1}$), where ϵ_{op} and ϵ_0 are the optical (infinite frequency) and static (zero frequency) solvent dielectric constants, respectively.[1] For polar solvents, $\epsilon_{op} \ll \epsilon_0$, since the latter quantity contains dominant additional contributions from orientational and vibrational solvent polarization; these components are absent in ϵ_{op} because only electronic polarization influences the solvent dielectric properties at optical frequencies. This circumstance leads to a numerical dominance of the Pekar factor, and hence the predicted ΔG^*_{os} values, in polar solvents by ϵ_{op} rather than ϵ_0. Perhaps paradoxically, then, the intrinsic reorganization energetics are anticipated to be influenced only mildly by the "slow" nuclear solvent modes.

In addition to such energetic factors, however, one might anticipate that such "slow" solvent repolarization as well as other nuclear reorganization modes that constitute the ET barrier could affect the reaction rate via their influence on the nuclear barrier-crossing frequency ν_n. This latter issue has been discussed most often recently for activationless (sometimes termed "solvent-controlled") ET reactions, where $\Delta G^* \approx 0$, so that the solvent relaxation dynamics alone determine the reaction rate. We focus here instead on *activated* ET processes, i.e., those featuring significant ($\gtrsim$2 kcal

† Dedicated to the memory of George E. McManis III.

0009-2665/92/0792-0463$10.00/0

mol^{-1}) free-energy barriers. While solvent dynamics can also exert important influences on the latter reaction type, the anticipated nature of the effects are often quite different from the activationless case.

In the usual transition-state theory (TST) format, one can express the (unimolecular) rate constant, k_{et}, for activated ET as[2]

$$k_{et} = \kappa_{el}\nu_n \exp(-\Delta G^*/k_B T) \quad (1)$$

where k_B is the Boltzmann constant, and κ_{el} is the electronic transmission coefficient. For sufficient donor–acceptor electronic coupling so that $\kappa_{el} \rightarrow 1$, "adiabatic" pathways prevail so that the ET barrier-crossing frequency will be controlled entirely by ν_n. The usual TST expression for ν_n is[2]

$$\nu_n = (\sum \nu_j^2 \Delta G_j^*/\Delta G^*)^{1/2} \quad (2)$$

where ν_j is the harmonic frequency of the jth nuclear mode which contributes to the overall barrier ΔG^* to an extent equal to ΔG_j^*. This expression indicates that the molecular rotational and other individual nuclear motions associated with solvent reorganization can influence ν_n and hence the reaction rate, although the form of eq 2 suggests that higher-frequency modes (especially vibrations) should often dominate ν_n. On this basis, the latter is anticipated to be the case for reactions where reactant intramolecular (i.e., inner-shell) distortions form a significant or substantial component of the activation barrier in addition to solvent (i.e., outer-shell) reorganization.

Over the last decade, however, it has become apparent that dynamical solvent properties can influence the rates of electron-transfer, as well as other chemical, processes in a distinctly more intricate and molecularly sensitive fashion. This recognition forms part of the broad-based theoretical development and associated experimental examination of so-called solvent "friction" effects in chemical kinetics.[3] The physical origin of these effects resides in the *collective* solvent motion which is encountered as a requirement for barrier crossing in many chemical processes, such as isomerizations and atom or group, as well as charge, transfers. The essential (albeit perhaps vague) general notion behind solvent friction is that this collective solvent motion impedes progress along the reaction coordinate below the TST rate (or frequency) characterizing the reactant subsystem itself. (This latter rate would, for example, be characterized by a bond frequency for atom transfers.) Rather than the solvent "bath" acting as an obedient reversible energy source or sink, as in the TST picture, *irreversible* reactant-solvent energy dissipation is perceived to occur, diminishing the net rate for passage up and over the barrier below the TST-anticipated value.[3] This frictional mode of passage along the reaction coordinate is often also termed "solvent diffusion" or "diffusive solvent motion". (It is important, however, not to confuse this meaning of "diffusion" with the common usage of the term describing, in a more macroscopic sense, mass transport in response to a concentration gradient.)

The physical nature of solvent friction in activated as well as activationless ET processes is somewhat different in that the solvent itself can form an important contributor to the reaction coordinate as well as provide the "energy bath", and indeed is the *sole* component of the activation barrier for reactions where reactant intramolecular distortions are absent. In this latter case, the "reactant mode" frequency for activated ET (and hence the free-energy well frequency ω_0) is related closely to the rotational time of individual solvent dipoles, τ_{rot}, in the dielectric medium. A simple TST formulation for this purpose is[4]

$$\nu_n = \frac{\omega_0}{2\pi} = (2\pi\tau_{rot}^g)^{-1}\left(\frac{2\epsilon_0 + \epsilon_\infty}{3\epsilon_\infty g_k}\right)^{1/2} \quad (3a)$$

$$= (2\pi\tau_{rot})^{-1} \quad (3b)$$

Here ϵ_∞ is the so-called "infinite frequency" dielectric constant and g_k is the Kirkwood "g" factor, both characterizing the solvent dielectric medium, and τ_{rot}^g is the "free" (gas-phase) solvent inertial rotation time which can be extracted from microwave spectra since $\tau_{rot}^g = (I/k_B T)^{1/2}$, where I is the molecular moment of inertia. The combined square-root term in eq 3a prescribes the alteration to the rotational time of individual solvent molecules induced by the surrounding dielectric medium, yielding the *solvent-phase* inertial rotation time τ_{rot} (eq 3b).

The presence of surrounding solvent molecules, however, can also diminish the effective frequency of the *collective* solvent motion required to move significantly along the ET reaction coordinate (and hence over the barrier top) well below this TST value, again by means of irreversible energy dissipation from the "reactant" solvent dipole to the surrounding solvent "bath". So-called "overdamped" solvent dynamics are obtained. This phenomenon, in general terms, encompasses the notion of "dielectric friction" by which the rates of ET processes can be impeded in polar media. While the familiar form of the TST-like expression eq 1 is still applicable formally under these circumstances [at least for $\Delta G^* \gtrsim (2\text{–}3)k_B T$], the rate will be depressed as a result of barrier-crossing frequencies, ν_n, which are smaller than the TST value, $\omega_0/2\pi$. For reaction barriers featuring significant contributions from intramolecular reactant (inner-shell) reorganization, dielectric friction can also act in a fashion more akin to other chemical processes by limiting the rate at which solvent configurations corresponding to reactant subsystem energies close to the barrier top are achieved, thereby impeding consequent barrier crossing via inner-shell motion (vide infra).

While the general notion of solvent-friction effects in chemical kinetics has its origins in a paper by Kramers published over a half-century ago,[5] theoretical development has occurred only much more recently. The initial application of dielectric-friction concepts to activated electron-transfer processes, by Zusman, appeared in 1980.[6] Since then, there has been a veritable deluge of analytic theoretical papers on this topic (see refs 7–15, along with recent reviews,[16] for a short representative selection). Related molecular-dynamical (MD) computational studies have also begun to appear.[17]

In the wake of this high degree of theoretical activity, it is of particular interest to explore experimentally the manner and extent of dynamical solvent effects on electron transfer in comparison with the theoretical predictions. Spawned by the recent development of ultrafast laser techniques, a number of studies of pho-

toinduced intramolecular charge-transfer reactions have been reported in which the rates appear to be dominated by the solvent dynamics, the reactions being close to activationless in nature.[18] Related measurements of time-dependent fluorescence Stokes shifts (TDFS) for chromophores forming suitable dipolar excited states have enabled the real-time dynamics of dipolar solvation to be examined directly.[18a,19] These remarkable measurements, involving in some cases subpicosecond time scales,[18a] have provided a detailed assessment of the strengths and limitations of both dielectric continuum and molecularly based models of overdamped solvent-relaxation dynamics. While providing invaluable experimental information on polar solvation dynamics of relevance to both activationless and activated ET processes, it is clearly also of importance to explore directly the possible roles of solvent dynamics on the latter class of reaction. The significance of this quest is highlighted by the knowledge that the vast majority of electron-transfer reactions are activated, i.e., feature free-energy barriers of several k_BT or more.

A central complication in exploring experimentally solvent dynamical effects for such activated processes, however, is that the measured rates are commonly influenced substantially (or even predominantly) by the activation energetics as well as dynamics, as reflected in the ΔG^* and ν_n terms, respectively, in eq 1. Consequently, the extraction even of semiquantitative estimates of the nuclear frequency factor from rate measurements requires reliable information on the activation energetics. At first sight, the evaluation of so-called activation parameters from temperature-dependent rate parameters might be expected to provide a straightforward separation of such preexponential and exponential kinetic factors. At least for bimolecular reactions, however, this approach often turns out to be far from unambiguous (see section VII).

In practice, most attempts to extract dynamical information for such activated processes utilize instead solvent-dependent rate measurements for electron-exchange processes (i.e., reactions in which $\Delta G^\circ = 0$).[20] The usefulness of this strategy derives from the expectation that in selected cases the anticipated solvent-dependent variations in ν_n, arising from differing solvent dynamics, are greater than, or functionally different from, those in the activation energetics factor $\exp(-\Delta G^*/k_BT)$. At least for judiciously chosen systems, this strategy can lead to the extraction of relatively reliable experimental information on solvent dynamical effects for homogeneous self-exchange and, to a lesser extent, for electrochemical exchange reactions.[20]

One specific aim of this article is to provide a critical assessment of the virtues and limitations of such experimental approaches, along with an overview of the dynamical information thus obtained in comparison with contemporary theoretical expectations. Of additional interest is the appraisal of such solvent dynamics for activated electron-transfer processes in relationship to the detailed knowledge of dielectric relaxation that has become available from ultrafast laser, as well as from solvent dielectric loss, measurements. Rather than attempt a comprehensive review of experimental and theoretical work in this multifaceted (and often esoteric) area, the overall emphasis here is on providing a (hopefully) straightforward and nonmathematical survey of the underlying physical concepts and experimental insight on solvent dynamical effects as they impact on our fundamental understanding of activated ET kinetics on a more general basis. A practical issue addressed herein is the degree to which solvent-dependent kinetic analyses can be utilized to gain *reliable* information of this type; unfortunately, as noted below, such procedures have been applied uncritically in some recent literature.

A briefer overview of some of these issues is to be found in ref 20. Attention is also drawn to several other recent reviews concerned with related experimental and conceptual aspects of dynamical solvent effects in charge-transfer phenomena.[15a,16b,18,19]

II. Conceptual Kinetic Framework

We consider here homogeneous-phase and electrochemical ET reactions, proceeding via outer-sphere mechanisms, having the general forms

$$Ox_1 + Red_2 \rightarrow Red_1 + Ox_2 \quad (4)$$

$$Ox_1 + \text{electrode (E)} \rightarrow Red_1 \quad (5)$$

where Ox and Red refer to oxidized and reduced forms of a given redox couple. Primary attention will be focused on homogeneous self-exchange processes (where $Ox_1 = Ox_2$, $Red_1 = Red_2$) and related electrochemical exchange reactions (for which the electrode potential E equals the standard potential E°). In both cases $\Delta G^\circ = 0$, thereby removing driving-force contributions to the activation barrier. Under these conditions, most of the conceptual discussion below applies interchangeably to both homogeneous-phase and electrochemical processes, although the distinct features of both reaction types will be emphasized whenever appropriate.

The observed rate constant, k_{ob}, for either homogeneous-phase or heterogeneous (electrochemical) ET processes can be related to the unimolecular rate constant in eq 1 most simply by[21,22]

$$k_{ob} = K_p k_{et} \quad (6)$$

where K_p is a preequilibrium constant which describes the statistical probability of finding the reactant (or reactant–electrode) pair in an internuclear configuration appropriate for reaction.[23] (This term can also contain appropriate electrostatic work-term corrections.) In general, a distribution of internuclear geometries, each having different formation probabilities (K_p) and "local" unimolecular rate constants (k_{et}), will contribute to k_{ob}, with the form of the required integral depending on the reactant geometries. Thus for a pair of "ideal spherical" reactants:[24]

$$k_{ob} = \left(\frac{4\pi N}{10^3}\right)\int_{r_o}^{\infty} r^2 k_{et}(r) g_{DA}(r)\, dr \quad (7)$$

where r is the reactant internuclear distance with r_o referring to contact, N is the Avogadro number, and g_{DA} is an appropriate radial distribution function. [A corresponding relation can be written for electrochemical processes, involving a single reactant (and a planar surface) by replacing the spherical with linear r coordinates.[25]] The g_{DA} term is usually set equal to unity, which is tantamount to assuming that the reactant electronic interactions (orbital overlap, etc.) exhibit simple spherical isotropy and that the solvent can be

perceived as a structureless continuum. (Examples where this is clearly not the case are considered below.) Even in the presence of molecular anisotropy, however, the observed bimolecular rate constant is often expected to reflect a sufficiently narrow range of precursor geometries so that the kinetics may be described approximately by singular values of k_{et}, ν_n, κ_{el}, ΔG^*, and K_p. Under these circumstances, eq 6 can provide a useful means of describing the observed rate constant. In this case, one can combine eqs 1 and 6 to yield the following overall expression for the electron-exchange rate constant, k_{ex}:

$$k_{ex} = K_p \kappa_{el} \nu_n \exp\left(\frac{-\Delta G_i^*}{k_B T}\right) \quad (8)$$

where ΔG_i^* is the "intrinsic" barrier (i.e., when $\Delta G^\circ = 0$).

This simplified formula provides a convenient starting point for outlining the basic features of solvent-dependent dynamical effects upon k_{ex} as anticipated from theoretical models, along with appropriate experimental analyses for exploring them. As already noted, the influence of solvent dynamics upon k_{ob} is contained within the nuclear frequency factor ν_n. The simplest case is where virtually the entire barrier arises from solvent reorganization, i.e., where the inner-shell contributions are small or negligible. Following the format of eq 3b, we can define an "effective" solvent relaxation time for barrier crossing, τ_{eff}, so that $\nu_n = (2\pi\tau_{eff})^{-1}$. In the presence of solvent friction (overdamped solvent relaxation), $\tau_{eff} > \tau_{rot}$, so that the observed reaction rate will fall below that expected for the TST limit.

Of central interest are the possible connections between τ_{eff} and the various solvent relaxation times observed in TDFS measurements or extracted from solvent dielectric loss spectra. For exchange reactions featuring a cusp (i.e., sharp) barrier top as expected for weak donor–acceptor electronic coupling, a dielectric-continuum treatment predicts that[6,7a,26]

$$\nu_n = \tau_L^{-1} (\Delta G_{os}^*/4\pi k_B T)^{1/2} \quad (9)$$

where ΔG_{os}^* is the intrinsic "outer-shell" barrier associated with solvent reorganization, and where τ_L is the well-known longitudinal solvent relaxation time. The latter is usually extracted from the Debye relaxation time, τ_D, obtained in dielectric-loss spectra by[27,28]

$$\tau_L = (\epsilon_\infty/\epsilon_0)\tau_D \quad (10)$$

From the form of eq 9, for reactions featuring moderate (say 4–8 kcal mol^{-1}) barriers as anticipated in polar solvents at ambient temperatures, $\nu_n \approx \tau_L^{-1}$, so that roughly $\tau_{eff} \approx \tau_L/2\pi$. For most common solvents at ambient temperatures, $\tau_L^{-1} < \tau_{rot}^{-1}$ and hence $\tau_L^{-1} < \omega_0$ (eq 3b). Some representative comparisons between τ_L^{-1} and ω_0 as estimated from eq 3 are contained in Table I.

Consequently, then, in the presence of such overdamped solvent relaxation one can anticipate commonly that $\tau_{eff}^{-1} \ll \tau_{rot}^{-1}$, so that significant rate retardations below the TST limit are usually expected on this basis. Additional inspection of Table I shows that, significantly, the τ_L^{-1} values are markedly more sensitive to the solvent nature than ω_0; for example, the former quantity is 20-fold smaller for benzonitrile than acetonitrile. This

TABLE I. Comparison between Inertial Frequencies Estimated from Eq 3 and Inverse Longitudinal Relaxation Times for Some Common Solvents at 25 °C

solvent	τ_L^{-1},[a] ps^{-1}	ω_0,[b] ps^{-1}
acetonitrile	4	11
D_2O	1.9	40
dimethyl sulfoxide	0.5	9.5
benzonitrile	0.2	4
hexamethylphosphoramide	0.11	~4
methanol	(0.135)	11
ethanol	(0.033)	9.5

[a] Inverse longitudinal relaxation times for solvent indicated, as obtained from dielectric loss data. (See ref 29 for data sources.) Values for methanol and ethanol (given in parentheses) refer to large amplitude, longer time, portion of multicomponent dielectric dispersion. [b] Estimates of solvent inertial frequency, extracted from eq 3. (See refs 4 and 30 for data sources.)

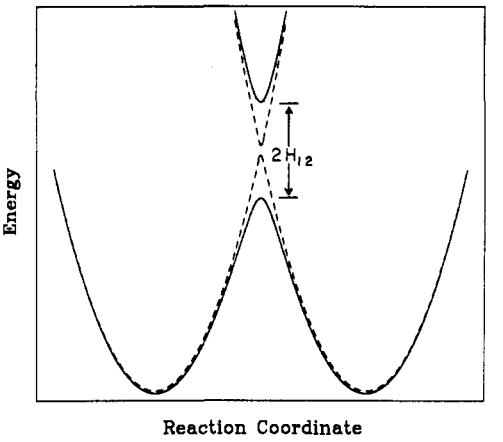

Figure 1. Schematic free energy–reaction coordinate profiles for symmetrical electron-transfer processes having small and large electronic matrix coupling elements, H_{12} (dashed and solid curves, respectively) (reprinted from ref 29; copyright 1989 American Chemical Society).

solvent structural sensitivity of τ_L, which is observed more generally,[29] suggests that the barrier-crossing frequency may be changed substantially by altering the solvent medium. A qualitatively similar conclusion can be reached on the basis of the solvation relaxation times, τ_s, extracted from TDFS measurements; comparisons between τ_L and τ_s will be considered further below. It is important to bear in mind that it is precisely this anticipated solvent dependence of the reaction dynamics that provides the basic experimental tactic utilized so far for exploring solvent-friction effects in activated ET processes.

Unlike the TST case, however, the barrier-crossing frequency in the presence of solvent friction is generally expected to be dependent not only on the barrier height ΔG_{os}^* (eq 9) but also on the shape of the barrier top. The latter is influenced by the degree of donor–acceptor orbital overlap as gauged by the electronic coupling matrix element, H_{12}; in the cusp-barrier limit, $H_{12} = 0$, with the barrier top becoming more "rounded" as H_{12} increases.[2] The relation between H_{12} and the ET barrier for a symmetrical exchange reaction is illustrated schematically in Figure 1. In the presence of solvent friction, ν_n is expected to diminish monotonically as the barrier-top roundedness increases.[7a,8c,30] For barrier shapes typical for activated outer-sphere ET, ν_n is predicted to be somewhat (ca. 2–5-fold) smaller than the cusp-limit value, ca. τ_L^{-1}, prescribed by eq 9.[30] Consequently, the degree of solvent friction commonly

expected for such ET processes will be somewhat greater than predicted by the oft-cited eq 9. A simple physical rationalization of this barrier-shape effect derives from the notion that solvent friction acts to diminish the net frequency factor ν_n in part by the barrier *recrossings*, or incomplete crossings, induced by such dissipative relaxation.[3a,b] As the barrier top broadens, therefore, the frequency of successful diffusive passages through this region should become progressively smaller. A simple, yet effective, treatment by Hynes[8c] sets the inverse net barrier-crossing frequency equal to the reciprocal sum of the rates for ascending the reactant well, k_w, and traversing the barrier top, k_b. Although both k_w and k_b can be diminished in the presence of solvent friction; the latter diminishes as H_{12} increases and is thereby more likely to become rate controlling under these conditions.

On the basis of the foregoing, then, there is reason to believe that rate measurements for suitable electron-exchange reactions in a judiciously chosen series of solvents should yield substantial insight into the nature and extent of dynamical solvent effects, providing that sufficient information is available on the solvent-dependent ET barrier heights. This notion is indeed borne out under some circumstances. Prior to discussing further the virtues and pitfalls of such solvent-dependent analyses, it is necessary to consider several additional features which together may conspire to make the influence of solvent dynamics on the reaction rate rather more involved than suggested by relations such as eq 9. The most important of these factors will now be briefly described in turn.

A. High-Frequency Solvent Dispersions. Even within the dielectric continuum limit, many solvents exhibit additional dispersions in the dielectric loss spectra at higher frequencies than the "major" Debye relaxation, τ_D.[27] In such cases, the relaxation dynamics are nonexponential and no longer described entirely by τ_L as extracted from eq 10. The observation of such "non-Debye" behavior in dielectric loss spectra has undoubtedly been limited by the frequency ranges over which such measurements have commonly been undertaken,[27] so that its occurrence may be much more common than is apparent from published data. Nevertheless, the clear observation of such high-frequency dissipative relaxations has been made in a number of solvents, most notably in primary alcohols.[31]

B. Noncontinuum (Solvent Molecularity) Effects. Even in the absence of multiple dissipative components for the pure solvent, there are good reasons to anticipate that τ_L can provide only an incomplete description of solvent relaxation in the vicinity of the reacting solute. Part of this evidence is derived from a number of theoretical examinations of "solvent molecularity" effects emanating from the inevitable limitations of dielectric-continuum treatments for describing local solvation. A simple approach for considering such molecular solvation effects is to utilize the mean spherical approximation (MSA) which treats the solvent as hard spheres with imbedded dipoles. A number of recent theoretical examinations along these lines stemmed from the demonstration by Wolynes that the MSA model could be utilized in a nonequilibrium fashion to treat the dynamics and energetics of solvent-controlled reactions.[7b] This approach applied to Debye solvents yields a spatial distribution of solvent relaxation times, increasing from τ_L far from the reacting solute to values close to τ_D at short distances.[7b,10b] (This spatial dependence was predicted originally by Onsager in 1977.[32])

There has been considerable interest in comparing such dynamical MSA predictions with experimental TDFS relaxation times, τ_s (see refs 18a and 19a,b for recent reviews). While initial comparisons suggested that $\tau_s > \tau_L$ in accordance with MSA predictions,[33] it now appears that the observed TDFS behavior is closer to the dielectric-continuum predictions than expected from the MSA model.[18a,19a] One suggested reason for this surprising success of the continuum theory is it arises from a fortuitous compensation between the influence of solvent molecularity and dipole translational motion.[19a] As shown by van der Zwan and Hynes[8b] and latterly by Bagchi et al.,[15] solvent dipolar translational as well as rotational motion can contribute importantly to the relaxation dynamics under some conditions. However, the relative lack of success of the MSA model may well be due also to its inability to account for specific solvent–solvent interactions.

Of particular interest is the recent observation by Barbara et al. of "fast" (subpicosecond) relaxation components in a number of solvents by means of TDFS measurements using coumarin solute probes.[18a,34] Besides the translational motion just noted, there are several theoretical reasons to anticipate the presence of τ_s components markedly shorter than τ_L even in Debye media, arising from short-range solvation and accompanying field inhomogeneity.[35,36] The likely relevance of rapid relaxation components, arising from either non-Debye or short-range solvation, to ET barrier-crossing dynamics is considered below.

Also worth noting briefly here is the possibility of dynamical contributions associated from ionic-atmosphere effects. These arise from the need to reorganize additionally the ionic population around the redox centers in order for electron transfer to occur. A theoretical treatment has appeared recently.[8d] In principle, the ion translational motions required can slow the rate of barrier crossing even below that prescribed purely by overdamped solvent motion. In practice, however, the rate effects predicted from this treatment turn out to be small or negligible, at least for reactions having the degree of barrier-top roundedness (i.e., electronic coupling) required for the occurrence of adiabatic pathways (see below).

C. Reactant Vibrational Effects. As already noted, many activated ET processes feature significant or substantial barrier components associated with reactant vibrational or other intramolecular distortions, arising from the differences in reactant bond lengths and angles between the oxidized and reduced states. Given the anticipated common importance of solvent friction, a significant issue is the degree to which such effects might be muted in the presence of relatively high frequency vibrational relaxation. It is important to recognize that eq 2 above, prescribing the contributions of individual activation modes to ν_n, is inherently a TST expression, thereby requiring for its applicability that each dynamical component is underdamped.

A distinctly different situation is encountered, however, in the presence of *overdamped* solvent motion. A theoretical treatment describing this latter case has been developed recently by Marcus and co-workers.[9]

Some numerical consequences of their approach are considered further below. It is pertinent to note here that the influence of overdamped solvent relaxation upon ν_n is anticipated to be attenuated in the presence of high-frequency reactant modes, in a qualitatively similar fashion to the TST limiting case. Thus the presence of such a rapid underdamped reaction coordinate can provide facile additional channels for barrier passage once the reactant subsystem has reached the vicinity of the barrier top primarily by means of overdamped solvent motion. A key difference, however, is that the overdamped dynamics can exert a significant influence upon ν_n even in the face of a much faster underdamped vibrational coordinate, especially as the former component becomes much slower than the latter. This expectation is quite different to the TST case (vide infra).

D. Reaction Nonadiabaticity. We have so far only considered ET barrier-crossing dynamics in the so-called adiabatic limit, corresponding to $\kappa_{el} \rightarrow 1$ in eqs 1 and 8, where the donor–acceptor electronic coupling is sufficient so to oblige the system to remain on a single reaction hypersurface throughout the passage from reactants to products. For the relatively weak electronic coupling (i.e., small H_{12} values) often characterizing outer-sphere ET processes, however, significantly nonadiabatic processes are expected whereby the system is liable to traverse the transition-state region while remaining on the reactant surface. Indeed, in this regard the circumstances leading to eq 9, involving a cusp-like barrier along with reaction adiabaticity, are somewhat hypothetical.

Besides diminishing the ET reaction rate, the preponderance of such nonreactive "nonadiabatic" transitions can alter drastically the nature of the barrier-crossing dynamics. This is because, unlike the adiabatic limit where the net barrier-crossing frequency $\kappa_{el}\nu_n$ is determined by the dynamics of the various nuclear modes, reactive barrier crossing in the nonadiabatic limit is characterized by an essential *independence* of the rate toward the nuclear dynamics, $\kappa_{el}\nu_n$ being controlled instead by the value of H_{12}. Physically, this nonadiabatic barrier passage can be understood most simply in terms of a compensation between the rapidity of motion along the reaction surface and the time, Δt_i, spent within the intersection region of the reactant/product parabolas. The influence of faster nuclear dynamics, yielding more frequent passage through the intersection region, will be nullified by a correspondingly smaller Δt_i each time, so that $\kappa_{el}\nu_n$ remains unaffected.

It is desirable to provide an algebraic means of interpolating appropriately between the adiabatic and nonadiabatic limits. In particular, accelerations in the nuclear dynamics as engendered by suitable alterations in the solvent medium (such as increasing τ_L^{-1}) are commonly expected to decrease the degree of reaction adiabaticity, and hence diminish the extent to which ν_n is affected by solvent dynamics. Consequently, then, the solvent-dependent rate behavior that is commonly utilized to explore solvent dynamics can be affected greatly by nonadiabatic effects.[25,29,37] A detailed discussion of appropriate interpolation formulas is provided in ref 25; in particular, a treatment was developed which accounts for the coupled influences of nonadiabaticity and barrier-top shape effects upon $\kappa_{el}\nu_n$.

For the present illustrative purposes, a useful expression is the simplified Landau–Zener formula:[2b,25]

$$\kappa_{el} = 2[1 - \exp(-\nu_{el}/2\nu_n)]/[2 - \exp(-\nu_{el}/2\nu_n)] \quad (11)$$

where the "electronic frequency factor" ν_{el} is given by

$$\nu_{el} = (H_{12})^2(\pi^3/\Delta G^* h^2 k_B T)^{1/2} \quad (11a)$$

where h is Plank's constant. For large H_{12} (i.e., strong electronic coupling), $\nu_{el} \gg \nu_n$ so that $\kappa_{el} \rightarrow 1$ in eq 11, and the nuclear dynamics term ν_n in eqs 1 and 8 controls entirely the barrier-crossing frequency. On the other hand, for weaker coupling so that $\nu_{el} \ll \nu_n$, eq 11 reduces to $\kappa_{el} \approx \nu_{el}/\nu_n$. For such latter "nonadiabatic" circumstances (corresponding to $\kappa_{el} \ll 1$), as already noted, the combined preexponential factor $\kappa_{el}\nu_n$ in eqs 1 and 8 will be *independent* of the nuclear dynamical term ν_n, equaling ν_{el} instead; i.e., proportional to $(H_{12})^2$ ("Golden Rule" limit).

III. Solvent-Dependent Kinetic Analyses: Separation of Dynamical and Energetic Factors

Having outlined some key physical factors that are anticipated to influence the nature of solvent dynamical effects in activated ET processes, we now consider in critical illustrative fashion some solvent-dependent kinetic analyses commonly utilized to extract dynamical information from experimental rate data. Experimental data for self-exchange reactions largely involving metallocenium–metallocene redox couples will be marshalled for this purpose, in view of the uniquely detailed kinetic, energetic, and electronic structural information available for these solvent dynamical reactant probes.[20] The central issue, and difficulty, involve the separation of the dynamical and energetic components, ν_n and ΔG^*, respectively, in eq 8, together responsible for the observed solvent-induced variations in k_{ex}. (This presupposes that electrostatic work terms and other K_p components are negligible or otherwise solvent independent.) A selection of publications from various laboratories (other than Purdue) where solvent-dependent rate data have been evaluated and analyzed for this purpose, for homogeneous self-exchange and electrochemical exchange processes, are given in refs 38 and 39, respectively.

The simplest approach used involves the assumption that the observed rate–solvent dependencies are due chiefly to the dynamical component, thereby neglecting the solvent dependence of ΔG^*. There are good reasons, however, to expect that the solvent-dependent dynamical and energetic components are often of roughly comparable magnitude. The latter, intrinsic outer-shell barrier, contribution is usually estimated by means of the following pair of well-known relations, for homogeneous and electrochemical reactions, respectively, derived from the dielectric-continuum theory:[1]

$$\Delta G^*_{os,h} = (e^2/4)(a^{-1} - R_h^{-1})(\epsilon_{op}^{-1} - \epsilon_0^{-1}) \quad (12)$$

$$\Delta G^*_{os,e} = (e^2/8)(a^{-1} - R_e^{-1})(\epsilon_{op}^{-1} - \epsilon_0^{-1}) \quad (13)$$

Here e is the electronic charge, a is the (spherical) reactant radius, R_h is the internuclear distance in the homogeneous-phase precursor state, and R_e is the corresponding distance between the reactant and its image in the metal electrode.

A key issue is the extent to which eqs 12 and 13 can provide reliable indicators of at least the *variations* in ΔG^*_{os} with the solvent. There are several limitations to the application of these relations, not the least of which are the inevitable uncertainties in the appropriate values of the "geometric factors" ($a^{-1} - R_h^{-1}$) and ($a^{-1} - R_e^{-1}$), expecially for nonspherical reactants. Moreover, there is theoretical evidence, supported by some experimental kinetic data, to suggest that the "imaging" (R_e^{-1}) term in eq 13 can even be qualitatively inappropriate.[40] The situation, however, for homogeneous-phase processes is somewhat less cloudy, due primarily to the additional availability of *experimental* estimates of ΔG^*_{os}, derived from optical ET energies, ΔE_{op}, observed for intramolecular redox systems.[41] For symmetrical valence-trapped binuclear systems,[41] $\Delta G^*_i = \Delta E_{op}/4$; this simple relation therefore enables the intrinsic outer-shell barrier ΔG^*_{os} in a given solvent to be obtained reliably if the inner-shell component is small or negligible. Provided that the binuclear system represents a close structural analogue of the bimolecular self-exchange reaction under study, then, such optical ET data can both circumvent the need to employ theoretical relations such as eq 12 and also furnish experimental tests of their applicability.

So far, little application of this tactic has been availed in solvent-dependent rate studies. An interesting example along these lines, which has undergone recent detailed examination in our laboratory, involves homogeneous self-exchange for metallocenium–metallocene redox couples, of the general form $Cp_2Co^{+/0}$ or $Cp_2Fe^{+/0}$, where Cp is a cyclopentadienyl ring (or derivative thereof).[20] By appropriate derivatization of the Cp ring along with metal substitution, a series of self-exchange reactions can be examined that feature systematic differences in the donor–acceptor electronic coupling.[29,42] Moreover, the redox couples feature small inner-shell barriers and can be examined in a range of solvents, k_{ex} being evaluated conveniently by proton NMR line-broadening techniques.[29,43] Solvent-dependent measurements of ΔE_{op} have also been undertaken for several binuclear ferrocenium–ferrocene ($Cp_2Fe^{+/0}$) complexes, yielding relatively reliable ΔG^*_{os} estimates for the $Cp_2M^{+/0}$ self-exchange reactions.[44]

Figure 2 consists of an illustrative comparison of solvent-dependent optical ΔG^*_{os} values with the corresponding theoretical estimates extracted from eq 12 in a series of 11 Debye (or near-Debye) polar solvents having known τ_L values. The former values (filled circles) were obtained as noted above for the bis(ferrocenyl)acetylene cation;[44] the latter theoretical estimates (open circles) were calculated as noted in ref 43a. (See figure caption for further details; note that the optical ΔG^*_{os} values probably contain a small, ca. 0.5 kcal mol^{-1}, contribution from inner-shell reorganization.[44]) The plot of $\Delta G^*_{os}/2.3RT$ versus log τ_L^{-1} shown in Figure 2 (for T = 298 K) is suggested by rewriting eq 8 in the form

$$\log \kappa_{el}\nu_n = \log k_{ex} - \log K_p + (\Delta G^*_{os}/2.3RT) \quad (14)$$

where ΔG^*_{is} is assumed to be negligible. This relation indicates that the reliability by which the required solvent-dependent dynamical factor $\kappa_{el}\nu_n$ can be extracted from rate-solvent measurements depends on the relative variations in log ν_n versus those in $\Delta G^*_{os}/2.3RT$, provided that κ_{el} and K_p remain constant.

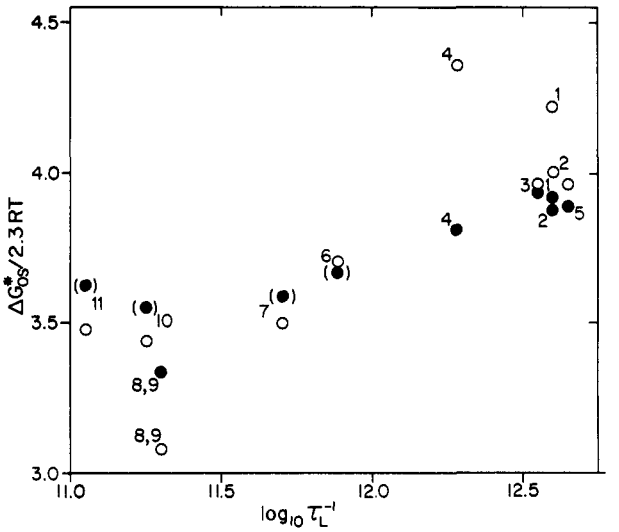

Figure 2. Plot of dimensionless barrier heights, $\Delta G^*_{os}/2.3RT$ (T = 298 K) for metallocene self-exchanges versus logarithm of inverse longitudinal relaxation time for 11 polar "Debye" solvents. Open circles are barrier heights obtained from dielectric-continuum formula (eq 12) with a = 3.8 Å, $R_h = 2a$. Filled circles are barrier heights extracted from optical electron-transfer energies, ΔE_{op}, for bis(ferrocenyl)acetylene cation, by $\Delta G^*_{os} = \Delta E_{op}/4$. Latter values given in parentheses are obtained by interpolation. (See refs 29, 43, and 44 for more details.) Key to solvents as given in caption to Figure 4.

Inspection of Figure 2 reveals several features of interest in this regard. Both the optical and theoretical ΔG^*_{os} values depend systematically on log τ_L^{-1}, so that the rate enhancements expected in dynamically more rapid solvents tend to be partially offset by the occurrence of correspondingly higher activation barriers (larger ΔG^*_{os}). This rough correlation between ΔG^*_{os} and log τ_L^{-1} is commonly observed in polar Debye media. It can be rationalized physically by noting that larger solvent molecules, yielding longer τ_L values, tend to be more polarizable, thereby also exhibiting larger ϵ_{op} and hence smaller ΔG^*_{os} values when (as for polar solvents) $\epsilon_{op}^{-1} \gg \epsilon_0^{-1}$ (eq 12). (Somewhat different behavior is encountered in relatively nonpolar media; as noted below, however, their use in solvent-dependent analyses suffers from several pitfalls.) In addition, while the optical ΔG^*_{os} values are typically close to (within ca. 0.4 kcal mol^{-1}) the corresponding theoretical ΔG^*_{os} estimates, Figure 2 shows that the former values are significantly less dependent on log τ_L^{-1} than are the latter. Possible origins of these small or moderate discrepancies have been discussed in terms of various extant molecular-based models of solvent reorganization; interestingly, the hydrogen-bound solvents water and methanol display the greatest deviations, whereby the optical ΔG^*_{os} values are about 15–25% below the continuum predictions.[44]

These systematic disparities between the optical and theoretical ΔG^*_{os} values yield noticeably different log ν_n – log τ_L^{-1} dependencies as inferred from the observed rate–solvent behavior, depending on whether the correction for the solvent-dependent barriers by means of eq 14 utilize the optical or theoretical ΔG^* values.[43b] An illustration of the numerical consequences for estimating the solvent-dependent preexponential factor is provided for ferrocenium–ferrocene self-exchange in Table II. The barrier-crossing frequencies labeled $\kappa_{el}\nu_n$(op) were obtained from the experimental k_{ex} values

TABLE II. Barrier-Crossing Frequencies, $\kappa_{el}\nu_n$ (s^{-1}), for Ferrocenium–Ferrocene Self-Exchange in Various Solvents as Estimated from Rate Data by Using Theoretical Dielectric Continuum, Compared with Experimental Optical, Barrier Heights

solvent	k_{ex},[a] M^{-1} s^{-1}	ΔG^*_{con},[b] kcal mol^{-1}	ΔG^*_{op},[c] kcal mol^{-1}	τ_L^{-1},[d] s^{-1}	$\kappa_{el}\nu_n$(con),[e] s^{-1}	$\kappa_{el}\nu_n$(op),[f] s^{-1}
acetonitrile	9×10^6	6.35	5.35	$\sim 3 \times 10^{12}$	1.5×10^{12}	3.0×10^{11}
propionitrile	9.2×10^6	6.05	5.15	$\sim 3 \times 10^{12}$	1.0×10^{12}	2.2×10^{11}
acetone	8×10^6	6.0	5.4	3.5×10^{12}	8×10^{11}	4.5×10^{11}
nitromethane	1.2×10^7	6.0	5.3	4.5×10^{12}	1.2×10^{12}	3.7×10^{11}
dimethyl sulfoxide	9.5×10^6	5.4	(4.9)	5×10^{11}	3.5×10^{11}	1.5×10^{11}
benzonitrile	2.7×10^7	4.8	4.55	2×10^{11}	3.5×10^{11}	2.4×10^{11}
nitrobenzene	3.0×10^7	4.8	4.55	2×10^{11}	4.0×10^{11}	2.6×10^{11}
methanol	1.8×10^7	6.45	5.2	(1.3×10^{11})	3.9×10^{12}	4.7×10^{11}
propylene carbonate	1.2×10^7	5.85	5.25	(4×10^{11})	8.5×10^{11}	3.4×10^{11}

[a] Rate constant for ferrocenium–ferrocene self-exchange (at ionic strength $\mu \simeq 0.01$–0.02 M), from ref 29. [b] Barrier height estimated from dielectric continuum formula (eq 12), by using $a = 3.8$ Å, $R_h = 2a$. (See refs 29 and 43 for other details.) An inner-shell contribution, estimated to be ca. 0.6 kcal mol^{-1}, is included.[29] [c] Barrier height obtained from experimental optical energies ΔE_{op} for bis(ferrocenyl)-acetylene cation in given solvent (see ref 44). Value in parentheses for DMSO is estimated by interpolation.[29] [d] Inverse longitudinal relaxation time of solvent, taken from compilation in ref 29. Values in parentheses are for solvents that exhibit additional higher-frequency dispersions. [e] Estimate of barrier-crossing frequency in given solvent, obtained from k_{ex} value by using eq 14, assuming that $K_p = 0.25$ M^{-1} and setting the barrier height equal to the dielectric-continuum estimate ΔG^*_{con}. [f] Barrier-crossing frequency, obtained as in footnote e, but by using the optical barrier height ΔG^*_{op} in each solvent.

and optical barrier heights, ΔG^*_{op}, also given in Table II, by means of eq 14.[45] (The preequilibrium constant, K_p, was taken to be 0.25 M;[46a] see refs 29 and 44 for data sources.) Listed alongside are corresponding barrier-crossing frequencies, $\kappa_{el}\nu_n$(con), extracted from the k_{ex} values in the same manner but utilizing instead barrier heights, ΔG^*_{con}, estimated by using the dielectric-continuum formula eq 12. (See ref 43a for most details; 0.6 kcal mol^{-1} was added to the ΔG^*_{os} values obtained from eq 12 to allow for the anticipated inner-shell barrier component.[29]) Also listed in Table II are the inverse longitudinal relaxation times, τ_L^{-1}, for each solvent (from ref 29). (Note that the last two entries, for methanol and propylene carbonate, are given in parentheses since these "non-Debye" solvents exhibit additional relaxation components at higher frequencies.)

Comparison between the $\kappa_{el}\nu_n$(con) and $\kappa_{el}\nu_n$(op) values for the sequence of polar solvents in Table II shows that while the former appear to correlate with τ_L^{-1} in the Debye media (albeit with a fractional slope), the latter are approximately *independent* of the solvent dynamics.[43b,45] Quite apart from the anticipated greater reliability of the $\kappa_{el}\nu_n$(op) values, being based on experimental rather than theoretical barrier estimates, there is good reason to anticipate that the $\kappa_{el}\nu_n$ for $Cp_2Fe^{+/0}$ self-exchange is indeed largely independent of the nuclear dynamics. Thus the calculated electronic matrix coupling elements for this reaction are sufficiently small[47] so that largely nonadiabatic pathways are expected to be followed throughout the range of solvent friction encountered in Table II.[29] (Such weak electronic coupling for $Cp_2Fe^{+/0}$ self-exchange is also consistent with recent gas-phase rate data.[48]) As noted above (eq 11), this circumstance (where $\kappa_{el} \ll 1$) will yield combined preexponential factors $\kappa_{el}\nu_n$ that approach *independence* of the nuclear component ν_n, in accordance with the observed $\kappa_{el}\nu_n$(op) values. The $\kappa_{el}\nu_n$(op) values are also in most cases markedly smaller than τ_L^{-1}, as expected on the basis of eq 9 if $\kappa_{el} \ll 1$.[49] For $Cp_2Co^{+/0}$ and other metallocene self-exchange reactions featuring stronger electronic coupling, however, $\kappa_{el}\nu_n$(op) correlates well with τ_L^{-1} under these conditions, indicating not only that adiabatic pathways are being followed, but the overdamped solvent relaxation model is appropriate under these conditions (see further discussion below).[29,43c]

The systematic observed dependence of the $\kappa_{el}\nu_n$(con) values upon τ_L^{-1} (Table II), on the other hand, would suggest that the reaction is somewhat adiabatic in nature. This, we think false, deduction arises from the systematically greater enhancements in the theoretical compared with the optical ΔG^*_{os} values as τ_L^{-1} increases (Figure 2), thereby yielding excessively large solvent-dependent barrier corrections. Consequently, then, the uncritical application of dielectric continuum estimates of ΔG^*_{os} in such solvent dynamical analyses can face difficulties for quantitative purposes. (This point is considered further below.)

Nevertheless, it turns out that the use of such theoretical barrier estimates, usually necessitated by the lack of experimental data, can yield valuable information on solvent-dynamical effects *if used with caution*. Three related graphical analyses of solvent-dependent rate data (labeled here as methods I–III) have commonly been utilized for this purpose. A simple strategy is to plot log k_{ex} versus the solvent Pekar factor $(\epsilon_{op}^{-1} - \epsilon_0^{-1})$ [46,51,52] (method I). In view of eqs 12–14:

$$\log k_{ex} = \log \kappa_{el}\nu_n + \log K_p - C(\epsilon_{op}^{-1} - \epsilon_0^{-1}) \quad (15)$$

where C is a constant which depends in part upon the precursor-state geometry (eqs 12 and 13). Despite the inevitable limitations of the dielectric-continuum model in estimating ΔG^*_{os}, evidence from optical data[41] indicates that ΔG^*_{os} in polar media at least correlates approximately with $(\epsilon_{op}^{-1} - \epsilon_0^{-1})$. From eq 15, then, log k_{ex} should diminish linearly as $(\epsilon_{op}^{-1} - \epsilon_0^{-1})$ increases, provided that $\kappa_{el}\nu_n$ remains largely solvent independent. This behavior has been observed for several homogeneous and electrochemical exchange processes.[51-53] Besides the occurrence of nonadiabatic pathways, such an insensitivity of $\kappa_{el}\nu_n$ to the solvent friction may often be anticipated in the presence of large inner-shell contributions to the barrier-crossing dynamics (see below).

However, in the presence of substantial solvent friction effects, such that $\kappa_{el}\nu_n$ becomes markedly dependent upon τ_L^{-1}, the slope of the log k_{ex} – $(\epsilon_{op}^{-1} - \epsilon_0^{-1})$ plot *can change sign*; since τ_L^{-1} roughly correlates with $(\epsilon_{op}^{-1} - \epsilon_0^{-1})$ in polar solvents (Figure 2, vide supra) the rate dimin-

utions with increasing Pekar factor can be more than offset by accompanying increases in log τ_L^{-1} (eq 15). Consequently, then, the observation of log k_{ex} – (ϵ_{op}^{-1} – ϵ_0^{-1}) plots having *positive* slopes (albeit with some scatter) can constitute reliable qualitative evidence of the presence of solvent-friction effects in the reaction dynamics.[46,52]

Providing that the geometric factors in eqs 12 or 13 controlling ΔG_{os}^* are known with some confidence, the energetic and statistical terms in eq 15 can be combined with the observed rate constant to yield an "observed" preexponential factor

$$\kappa_{el}\nu_n(\text{obs}) = k_{ex}[K_p \exp[-(\Delta G_{os}^* + \Delta G_{is}^*)/RT]]^{-1} \quad (16)$$

where the overall barrier height may include any "inner-shell" contribution, ΔG_{is}^*, arising from intramolecular reactant distortions. Examining plots of log $\kappa_{el}\nu_n$(obs) versus log τ_L^{-1}, or related dynamical quantities, (method II) can yield insight into the manner and extent to which the rates are influenced by solvent dynamics in suitable cases.[43a,57] Thus for processes controlled essentially by solvent dynamics, the plot slope should approach unity, whereas markedly smaller slopes are anticipated for reactions following nonadiabatic or other solvent-independent dynamical pathways. From the above discussion, the obvious limitation to this approach lies in the need to presume the correct form of the solvent-dependent barrier height. Method II is therefore most useful in situations where there is good reason to expect that the variations in the solvent dynamics are greater than in the energetics.

An alternative, yet related, approach for separating dynamical and energetic factors utilized in several studies[38d-h,50] (labeled here method III) involves rearranging eq 15 in the form

$$\log (k_{ex}/\kappa_{el}\nu_n) = \log K_p - C(\epsilon_{op}^{-1} - \epsilon_0^{-1}) \quad (17)$$

and assuming that ν_n is given by the "cusp-limit" continuum formula, eq 9. Provided that the solvent-dependent preexponential factor is indeed given by eq 9, having the functional form $\tau_L^{-1}(\epsilon_{op}^{-1} - \epsilon_0^{-1})^{1/2}$, a plot of log $[k_{ex}\tau_L(\epsilon_{op}^{-1} - \epsilon_0^{-1})^{1/2}]$ versus $(\epsilon_{op}^{-1} - \epsilon_0^{-1})$ should yield a negative slope having a value reflecting the energetic "geometric factor" C (eqs 15 and 17). This analysis (method III) is therefore the converse of method II, since these attempt to correct the solvent-dependent rate constants for the energetic and dynamical components, respectively.

Method III can also be useful for data analysis under some circumstances.[38d-h] It can, however, yield quite misleading results since unlike method II it *presumes* not only an oversimplified functional form of ν_n (i.e., $\alpha\ \tau_L^{-1}$) but also that the preexponential factor is controlled *entirely* by solvent dynamics. In the commonly anticipated cases where nonadiabatic, inner-shell, or non-Debye solvent dynamical effects are significant, method III is strictly invalid. Thus in the former limit, as noted above κ_{el} is not constant, as presumed in method III, but is inversely proportional to ν_n so that the combined term $\kappa_{el}\nu_n$ in eq 17 will be solvent independent. This key point was not appreciated in ref 50, for example, leading unfortunately to spurious estimates of energetic and preexponential statistical factors extracted from literature experimental data by means of method III.

It is appropriate here to comment on some experimental limitations of such analyses, especially for more quantitative purposes. First, for several reasons the dielectric-continuum treatment is inherently less reliable in weakly polar or nonpolar media (e.g., chloroform, dichloromethane, dioxane, etc.). The low ϵ_0 values (say $\lesssim$15) that characterize such media lead to greater uncertainties in the applicability of eqs 12 and 13 due to dielectric saturation and ion-pairing effects.[54] The former difficulty is recognized most simply by noting that in nonpolar media the "static" (Born charging) dielectric term ϵ_0^{-1} can make a substantial contribution to ΔG^* as estimated from eqs 12 and 13.[54c] Unlike the optical term, ϵ_{op}^{-1}, the magnitude of ϵ_0^{-1} is sensitive to dielectric saturation and related local solvation effects. The latter point is exemplified for dichloromethane in ref 54a, in which optical electron-transfer barriers for bis(ferrocenyl)acetylene cation are clearly shown to be very sensitive to the ionic strength as a result of ion-pairing effects. Such factors can also yield substantial uncertainties in electrostatic work terms, even for monocharged reactants.

The measurement of ET rate constants themselves can often suffer from systematic errors, especially for fast reactions, yielding apparent rate-solvent dependencies which give the false impression of displaying dynamical solvent effects. Thus rapid bimolecular ET reactions can easily be subject to at least partial rate control by reactant diffusional transport, rather than by activated electron transfer; diffusion rates are typically inversely proportional to the solvent viscosity, which in turn tends to correlate with solvent friction parameters. (Recall again, however, the distinction between solute mass transport by diffusion and diffusional motion *along the reaction coordinate*, i.e., solvent friction.) Additional difficulties along these lines are often anticipated for electrochemical rate measurements in nonpolar media. Such solvents tend to exhibit low conductances even in the presence of high supporting electrolyte concentrations, exacerbating the acquisition of reliable ET rate data. These problems can be particularly insidious since solvent conductivities (as well as diffusion coefficients) often correlate crudely with dielectric-friction parameters, so that failure to account properly for the former when evaluating the electrochemical rate parameters can yield apparent rate-solvent dependencies that infer incorrectly the presence of the latter effect. Unfortunately, the literature contains a number of examples of solvent-dependent rate data that almost certainly suffer from one or more of these difficulties, yielding misleading or even entirely incorrect information regarding perceived solvent-dynamical effects.

While the smaller Pekar factors commonly obtained for nonpolar solvents encourage their use in log k_{ex} – ($\epsilon_{op}^{-1} - \epsilon_0^{-1}$) and related analyses (for example, ref 38h), such tactics can be problematical. Indeed, some authors have regarded observed deviations from the anticipated negative log k_{ex} – ($\epsilon_{op}^{-1} - \epsilon_0^{-1}$) slopes as signaling breakdowns in the dielectric-continuum formulas themselves rather than to the appearance of solvent dynamical effects.[16c] While we do not agree entirely with this assessment, the desirability of restricting such solvent-friction analyses to polar media is clearly evident, at least for bimolecular or electrochemical electron-exchange reactions.

Another limitation of dynamical analyses based on relations such as on eq 15 is that it is usual to presume (as we have above) that the preequilibrium constant K_p is solvent independent. Aside from the possibility that K_p may contain solvent-specific work terms, for weakly adiabatic processes one anticipates generally that K_p will *diminish systematically* as τ_L^{-1} and hence ν_n increases.[25,29] The reasoning involved can readily be discerned from eqs 7 and 11. As τ_L^{-1} and hence ν_n increases, κ_{el} for each particular encounter geometry (corresponding to a given H_{12} value) will decrease, thereby shrinking the range of r-dependent geometries that contribute to the bimolecular rate constant (eq 7). The effective K_p will therefore diminish systematically as the nuclear dynamics becomes more rapid. A consequence of this effect, first discussed by Beretan and Onuchic,[55] is that use of the preequilibrium model, whereby K_p is assumed to be solvent-independent, tends to underestimate the effect of solvent-dependent dynamics upon k_{et}.[25] Stated equivalently, the k_{ex}-solvent-friction dependencies anticipated by taking into account such spatial integration tend to be noticeably smaller, and of different functionality, than those based on the simple preequilibrium model.[25]

Finally, it is appropriate to comment briefly on the limitations of multiparametric analyses of solvent dynamics based on simplified preequilibrium–dielectric continuum models. As mentioned above, the difficulty in separating dynamical and energetic factors according to method III is the a priori unknown solvent functionality of $\kappa_{el}\nu_n$. In a revised analysis, Fawcett et al.[56] allowed for this complication by setting $\kappa_{el}\nu_n$ proportional to $\tau_L^{-\alpha}$, where $0 \leq \alpha \leq 1$, leading to a relation of the form

$$\log k_{ex} = \log A - \alpha \log \tau_L - C(\epsilon_{op}^{-1} - \epsilon_0^{-1}) \quad (18)$$

where A is a largely solvent-independent term. These authors fitted solvent-dependent rate data to a multiparametric analysis to find essentially best-fit values of the "dynamical" and "energetic" terms α and C, respectively, that contribute to the observed rate–solvent dependencies. A number of inherent difficulties in this analysis can be gleaned from the above discussion. One problem lies in the tendency for the solvent-dependent dynamical and energetic terms to correlate with each other (Figure 2), hampering their reliable functional distinction unless one or the other is known independently. Admittedly, the correlation between $\log \tau_L^{-1}$ and $(\epsilon_{op}^{-1} - \epsilon_0^{-1})$ is typically not found in weakly polar (or nonpolar) solvents, which also can provide substantial variations in the latter term. As already noted, however, the use of the continuum formulas (eqs 12 and 13) to estimate ΔG_{os}^* is especially suspect in nonpolar media. Consequently, then, the use of such multiparametric analyses to diagnose and analyze solvent dynamical effects for weakly adiabatic process tend to be, in our opinion, specious rather than genuinely insightful. We comment further on related semiempirical analyses of solvent effects in section VIII below.

IV. Quantitative Assessment of Solvent-Friction Effects

The foregoing discussion, focusing on the problems of accounting for energetic and other obfuscating factors in rate–solvent dynamical analyses, may understandably give the impression that the experimental dissection of such phenomena is fraught irrevocably with pitfalls. While this can be the case, enough reliable data has now been assembled to allow some broad-based, even quantitative, conclusions to be reached. A number of studies of electrochemical exchange reactions have been reported in this context, involving inorganic,[52,57] organometallic,[46,58] and organic radical redox couples.[39] In most cases, at least qualitative evidence was obtained for the presence of a solvent-dependent prefactor correlating with τ_L^{-1} in Debye-like media. These results support the notion that the electrochemical reactions are commonly adiabatic, the dynamics being controlled at least partly by overdamped solvent relaxation. An interesting exception is provided by the electron exchange of tris(hexafluoroacetylacetonato)rutheium-(III)/-(II), for which the electrochemical as well as homogeneous-phase kinetics display $\log k_{ex} - (\epsilon_{op}^{-1} - \epsilon_0^{-1})$ plots consistent with a solvent-independent prefactor.[51,52] The inferred nonadiabatic behavior can be rationalized on basis of the electronically "insulating" character of the large aliphatic ligands.[52]

In comparison with electrochemical systems, fewer homogeneous self-exchange reactions display clearcut evidence for adiabatic, solvent-friction-controlled, dynamics on this basis (e.g., see ref 38c). Nevertheless, the most quantitative dynamical information has been obtained from experimental data of this type. In particular, Grampp and co-workers have performed comprehensive kinetic measurements for organic radical redox couples in nonaqueous media by using ESR line-broadening techniques.[38] To illustrate the insight that can be obtained from such studies, we focus attention further on results obtained in our laboratory for solvent-dependent $Cp_2M^{+/0}$ self-exchanges. Unlike the electrochemical exchange reactions, the rates of these processes display an intriguing sensitivity to the metallocene electronic structure as well as the solvent.[29,42,43] A quantitative analysis of these rate variations, utilizing the optical barrier data noted above, provides insight into the role of donor–acceptor electronic coupling in the overall dynamics.

Figure 3 summarizes some key experimental data of this type, taken from ref 29, in the form of a plot of $\log k_{ex}'$ for five $Cp_2M^{+/0}$ couples in 11 Debye (or near-Debye) solvents, against $\log \tau_L^{-1}$. The "barrier-corrected" rate constants k_{ex}' [referring to a fixed (cusp) barrier height of 5.0 kcal mol^{-1}] were obtained from the measured k_{ex} values by correcting them for the solvent-dependent ΔG_{os}^* values (which range from ca. 4.6 to 5.4 kcal mol^{-1}). The remaining solvent-induced rate variations should largely reflect changes in dynamics rather than energetics. Inspection of Figure 3 shows that the $\log k_{ex}' - \log \tau_L^{-1}$ dependencies depend markedly on the metallocene couple. While k_{ex}' for the least facile, $Cp_2Fe^{+/0}$, reactants exhibit little dependence on τ_L^{-1}, the $\log k_{ex}' - \log \tau_L^{-1}$ slopes increase progressively for the more rapid $Cp_2Co^{+/0}$ systems as k_{ex}' in a given solvent increases. In a given solvent, the k_{ex} values vary by up to 100-fold. In addition, although there is significant scatter, the $\log k_{ex}' - \log \tau_L^{-1}$ slopes for a given reaction tend to decrease toward larger $\log \tau_L^{-1}$ values.

These observations are in harmony with expectations based on a consideration of variable donor–acceptor electronic coupling. For this purpose, Figure 4 displays

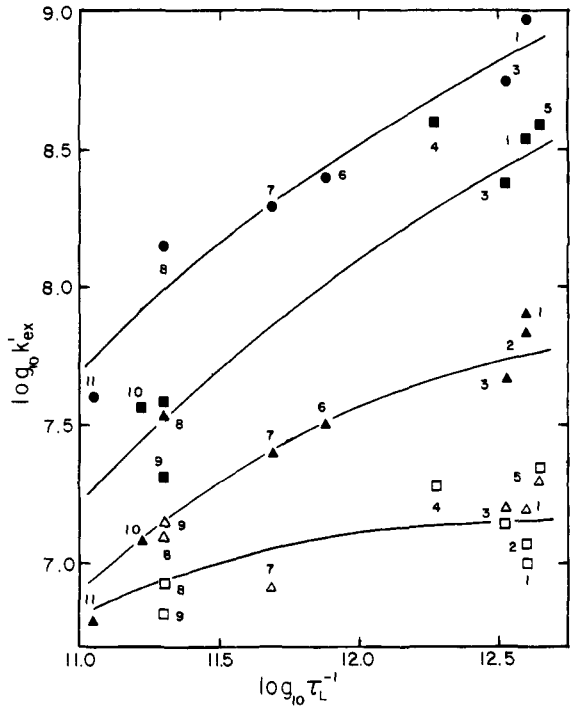

Figure 3. Logarithmic plots of "barrier-corrected" rate constants (M^{-1} s^{-1}, extracted from rate and optical barrier data) versus inverse longitudinal relaxation time (s^{-1}) for five metallocene self-exchange reactions in 11 solvents, taken from ref 29. See Figure 4 caption for key to solvents. Key to redox couples: filled circles, $Cp'_2Co^{+/0}$ (Cp' = pentamethylcyclopentadienyl); filled squares, $Cp^e_2Co^{+/0}$ [Cp^e = (carboxymethyl)cyclopentadienyl]; filled triangles, $Cp_2Co^{+/0}$; open triangles, $Cp_2Fe^{+/0}$; open squares, (hydroxylmethyl)ferrocenium/-ferrocene (reprinted from ref 29; copyright 1989 American Chemical Society).

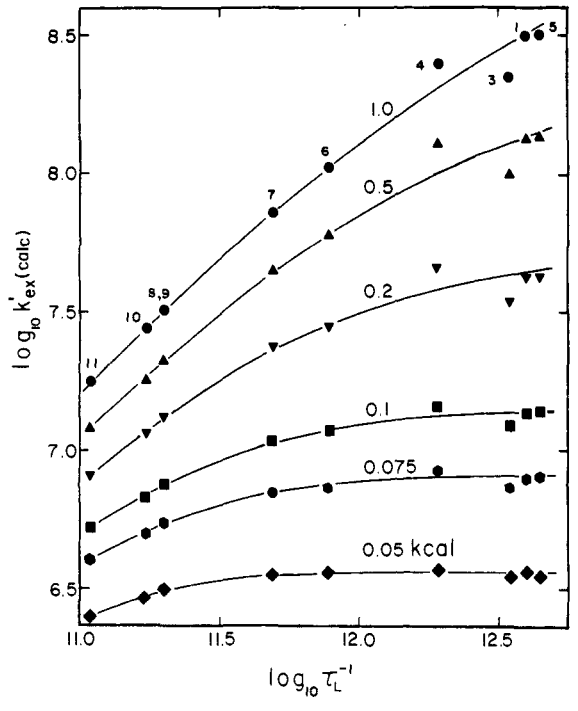

Figure 4. Logarithmic plots of calculated "barrier-corrected" rate constants (M^{-1} s^{-1}, for 5.0 kcal mol^{-1} "cusp" barrier), for electron self-exchange versus inverse longitudinal relaxation time (s^{-1}) in 11 "Debye" solvents for the sequence of six electronic coupling matrix elements (at reactant contact) as indicated. See ref 29 for details. Key to solvents: 1, acetonitrile; 2, propionitrile; 3, acetone; 4, D_2O; 5, nitromethane; 6, dimethylformamide; 7, dimethyl sulfoxide; 8, benzonitrile; 9, nitrobenzene; 10, tetramethylurea; 11, hexamethylphosphoramide (reprinted from ref 29; copyright 1989 American Chemical Society).

theoretical log k'_{ex} – log τ_L^{-1} plots (also taken from ref 29) computed for the same set of solvents as in Figure 3, for spherical reactants featuring the sequence of electronic coupling matrix elements, H^o_{12}, (referring to reactant contact), as indicated. The k'_{ex}(calc) values were calculated from conventional solvent-dynamical theory, taking into account both barrier-top shape effects and a spatial integration of bimolecular encounter geometries by using eq 7. The form of these log k'_{ex}(calc) – log τ_L^{-1} plots in Figure 4, closely similar to the experimental curves (Figure 3), can readily be understood in terms of eq 11. Thus enlarging H_{12} and/or τ_L will increase κ_{el} and hence the degree to which solvent dynamics, rather than nonadiabatic electron tunneling, controls the barrier-crossing frequency, as seen by the systematic increases in the log k'_{ex}(calc) – log τ_L^{-1} slopes under these conditions (Figure 4). [The scatter seen in Figure 4 for some low-friction solvents arises from the variable anticipated effects of solvent inertia, corresponding to the emergence of the TST limit (vide supra).[29]]

Significantly, Figure 4 shows that the appearance of substantial solvent friction effects requires the presence of relatively strong electronic coupling ($H^o_{12} \gtrsim 0.2$ kcal mol^{-1}) for the range of τ_L^{-1} values, ca. 10^{11} to 4×10^{12} s^{-1}, that characterize most polar Debye media at ambient temperatures. Further, the log k'_{ex}(calc) – log τ_L^{-1} slopes are significantly below unity even at the highest H_{12} and τ_L values encountered in Figure 4. This latter feature arises from the expectation of friction-dependent K_p values, as noted above. Intercomparisons betwen Figures 3 and 4 enable approximate estimates of H^o_{12} for the various metallocene self-exchange reactions to be obtained. These vary from about 0.1 kcal mol^{-1} for $Cp_2Fe^{+/0}$ to 0.5 kcal mol^{-1} for $Cp_2Co^{+/0}$ and 1.0 kcal mol^{-1} for $Cp'_2Co^{+/0}$ (Cp' = pentamethylcyclopentadienyl). Interestingly, the first two experimental H^o_{12} estimates are in approximate accord with the average values obtained for various metallocenium–metallocene precursor geometries by Newton et al.[47] The greater electronic coupling for the cobalt versus the iron metallocenes can be understood qualitatively in terms of the ligand- and metal-centered nature, respectively, of the molecular orbitals that participate in electron transfer.[42,47]

Overall, these and other experimental results indicate that overdamped solvent relaxation as described in Debye media by τ_L^{-1} can provide at least an approximate description of the nuclear barrier-crossing dynamics, even though substantial donor–acceptor electronic coupling is required in order to yield a dominant influence of solvent friction upon the reaction rate. The findings, however, certainly do not exclude the occurrence of significant deviations from the simple dielectric continuum picture associated with short-range solvent reorganization and other factors.

V. Influence of Rapid Solvent Relaxation Components

Given this largely satisfactory picture, it is of particular interest to explore the manner and extent to

TABLE III. Comparison between Inverse Solvent Relaxation Terms from Dielectric Loss and TDFS Data with Effective Barrier-Crossing Frequencies for Metallocene Self-Exchanges

solvent	ΔG^*,[a] kcal mol^{-1}	τ_L^{-1},[b] ps^{-1}	τ_S^{-1},[c] ps^{-1}	$\kappa_{el}\nu_n$, ps^{-1} [d]	
				$Cp^e_2Co^{+/0}$ [e]	$HMFc^{+/0}$ [f]
acetonitrile	5.35	~3	1.8	2.5	0.2
acetone	5.4	3.5	1.0 (53%) 3.5 (47%)	2	0.25
nitromethane	5.3	4.5		3	0.4
water	5.2	1.9	1.0 (50%) 4.0 (50%)	3.5[g]	0.35[g]
benzonitrile	4.55	0.17	0.16 (61%) 0.47 (39%)	0.3	0.15
nitrobenzene	4.55	0.19		0.15	0.12
propylene carbonate	5.25	(0.3)	0.24 (54%) 2.3 (46%)	1.5	
methanol	5.2	(0.13)	0.10 (60%) 0.9 (40%)	1.5	0.45

[a] Cusp free-energy barrier for self-exchange reactions, estimated from optical electron-transfer energies for bis(ferrocenyl)acetylene cation in indicated solvent. (See refs 29 and 44 for details.) [b] Inverse longitudinal relaxation time for solvent indicated, obtained from dielectric loss spectra. (See refs 20 and 29 for data sources.) [c] Inverse solvation times, along with percentage weighting factors, obtained from TDFS data for the coumarin C152 except for water which refers to C343 (refs 18a and 34). [d] Effective barrier-crossing frequency for metallocene self-exchange reaction indicated, obtained from experimental k_{ex} values together with listed ΔG^* values, assuming that $K_p = 0.25$ M^{-1} (Eq 14). See refs 29 and 61 for kinetic data and other details; ΔG^* values for $Cp^e_2Co^{+/0}$ taken to be 0.5 kcal mol^{-1} smaller to allow for electronic coupling.[29] [e] $Cp^e_2Co^{+/0}$ = (carboxymethyl)cobaltocenium/-cobaltocene [$(CpCO_2Me)_2Co^{+/0}$]. [f] $HMFc^{+/0}$ = (hydroxymethyl)ferrocenium/-ferrocene [$Cp(CpCH_2OH)Fe^{+/0}$]. [g] Rate data refers to D_2O.

which the presence of additional, more rapid, overdamped relaxation components may influence the barrier-crossing dynamics. At least the qualitative presence of such effects has been diagnosed in several cases, especially for primary alcohols, from the markedly (≳10-fold) higher k_{ex} values obtained for both organic[39d] and organometallic redox couples[30,43a,46b,61] in such alcohols in comparison with the rates in aprotic media yielding similar anticipated barriers. As mentioned above, primary alcohols contain significant dispersion components of the dielectric loss spectra at markedly (≳10-fold) higher frequencies than the major "Debye" relaxation.[31] However, the use of analyses employing dielectric-continuum ΔG^*_{os} estimates may well overestimate the importance of such effects, as adjudged by the markedly (ca. 0.5–1 kcal mol^{-1}) smaller ΔG^*_{os} values obtained for such hydrogen-bound solvents from optical data.[44]

Of particular interest is the comparison between the direct information on rapid solvent relaxation components obtained recently from subpicosecond TDFS measurements[18a,34] with data for adiabatic barrier-crossing dynamics in activated ET. Pertinent data extracted from the sole comparison along these lines reported so far[61] are summarized in Table III (taken from ref 20). The two far right-hand columns contain net barrier-crossing frequencies, $\kappa_{el}\nu_n$, in eight selected solvents extracted for a pair of metallocene self-exchange reactions from k_{ex} and optical ΔG^*_{os} data using the same procedure as in Table II. The redox couples, labeled $Cp^e_2Co^{+/0}$ [Cp^e = carboxymethyl)cyclopentadienyl] and $HMFc^{+/0}$ [(hydroxymethyl)-ferrocenium/-ferrocene] are selected since they display largely adiabatic and nonadiabatic behavior, respectively,[29] and can be examined in a range of solvents, including water.[43c]

Alongside these barrier-crossing frequencies are listed inverse relaxation times, τ_s^{-1}, for each solvent obtained from TDFS data for coumarin probes by Barbara et al.[34,61] Almost all these solvents display nonexponential decay behavior; the relaxation times and weighting factors resulting from biexponential fits are given in Table III, along with corresponding τ_L^{-1} values extracted from dielectric loss spectra. For the most part, the "longer-time" τ_s^{-1} components are comparable (within ca. 2-fold) to the corresponding τ_L^{-1} values. Two of the solvents, propylene carbonate and methanol, exhibit discernable "shorter-time" dielectric-loss components; the predominant "long-time" τ_L^{-1} values are given in parentheses in Table III.

Similar to $Cp_2Fe^{+/0}$ self-exchange (Table II, vide supra), the $\kappa_{el}\nu_n$ values for $HMFe^{+/0}$ are uniformly smaller than τ_L^{-1} or τ_s^{-1} and are insensitive to the solvent dynamics, as expected for a nonadiabatic process. For $Cp^e_2Co^{+/0}$, however, the $\kappa_{el}\nu_n$ values not only correlate well with the solvent relaxation dynamics, but are also uniformly close to (within 1.5-fold) the *faster* τ_s^{-1} component (Table III). Admittedly, this agreement between the *absolute* $\kappa_{el}\nu_n$ and τ_s^{-1} values is probably fortuitous given the inevitable uncertainties in extracting the former. The observed close correlation nevertheless demonstrates the importance of the more rapid dynamical component in accelerating the ET barrier-crossing frequency. The findings for methanol and water are perhaps of greatest interest.[43c,61] The influence of the high-frequency relaxation in methanol is especially striking, yielding barrier-crossing frequencies that approach those in water and other low-friction media despite the presence of a markedly (10–30) longer τ_L value. Comparable findings have been obtained for other adiabatic metallocene reactions.[29,30,43] Despite these substantial rate accelerations, most of the inferred $\kappa_{el}\nu_n$ values are still significantly smaller than would correspond to the anticipated inertial (i.e., TST) limit, as can be gauged by comparing the $\kappa_{el}\nu_n$ values with the $\omega_0/2\pi$ estimates obtained from Table I.

The issue of the degree to which such rapid overdamped relaxations can enhance ET rates has been the subject of substantial theoretical interest (see ref 30).[8c,10a,14a,b,62] In particular, a treatment by Hynes,[8c] which considers dynamical effects in both reactant well and barrier-top regions, yields predictions largely in accord with these experimental observations: even relatively small amplitude rapid relaxations can yield

substantial rate accelerations.[30,61] This deduction, based on analytic theory, is also in harmony with the results of numerical simulations utilizing a cusp barrier.[63] The degree to which the rapid dynamical components accelerate ν_n is predicted to diminish somewhat as the donor–acceptor coupling (H_{12}) increases, so that the barrier top becomes more "rounded".[8c,30] This effect arises from the increased influence that overdamped relaxation in the barrier-top region, rather than in the wells, is expected to exert under these conditions. Nevertheless, numerical calculations suggest that the accelerating role of higher-frequency relaxations remains marked even at large H_{12} values, around 1 kcal mol^{-1}.[30] Dipole *translation*, as well as rotational, motion is also predicted to contribute to the rapidity of the TDFS and barrier-crossing dynamics in methanol.[8b,61]

The common presence of very rapid (say $\tau_s \lesssim 0.1$ ps), overdamped relaxation even in supposedly "Debye" media, has also been suggested by several recent molecular dynamical (MD) simulations.[19a] Besides the numerical value of such calculations, they can provide interesting insight into the physical origins of solvent relaxation. So far, most solvents examined (e.g., water, acetonitrile) constitute relatively low-friction media, where the role of solvent inertia is relatively important in the overall dynamics.[19a] It would clearly be of substantial interest to pursue MD simulations for solvents where overdamped relaxation is anticipated to be more dominant.

VI. Influence of Reactant Intramolecular Dynamics

Up to this point, we have considered dynamical solvent effects for experimental ET systems where the activation barrier is known (or believed) to arise wholly or predominantly from dipolar solvent reorganization. A much more common circumstance, however, involves the presence of barrier components from reactant intramolecular (inner-shell) reorganization that are comparable to, or larger than, the solvent contribution. Given that the frequencies of such intramolecular motions, especially vibrational modes, are usually anticipated to be higher than for solvent overdamped or even inertial motion, one might anticipate that the barrier-crossing frequency would commonly be dominated by inner-shell rather than solvation dynamics. As mentioned above, this conclusion indeed commonly applies in the TST limit, as prescribed by eq 2. A rather different situation might be anticipated in the presence of solvent friction: even though the presence of higher-frequency inner-shell distortions should accelerate barrier passage, the reaction rate may be limited in part by a slow diffusive approach toward the barrier top. Despite its practical importance, relatively little attention has been devoted to this issue. Nevertheless, a detailed theoretical treatment for cusp barriers, spanning the range from activationless to activated ET processes, has been outlined by Marcus and co-workers.[9]

Some numerical consequences of their treatment for activated ET processes are illustrated in Figure 5. This consists of a plot of log k_{ex} for a model electron-exchange reaction[64] versus the inner-shell barrier ΔG^*_{is}, with the outer-shell barrier held at 4.0 kcal mol^{-1}. Both

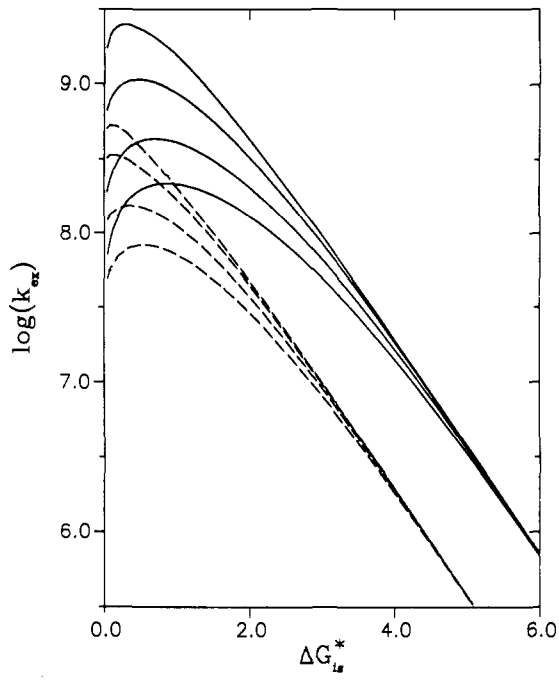

Figure 5. Illustrative plot of logarithm of unimolecular rate constant for model electron-exchange reaction, k_{ex} (s^{-1}), versus the inner-shell barrier, ΔG^*_{is} (kcal mol^{-1}), in the presence of varying overdamped solvent dynamics, as calculated[65] from treatment based largely on Marcus et al.[9] Outer-shell barrier is held at 4.0 kcal mol^{-1}; solvent inertial frequency $\omega_0 = 1 \times 10^{13}$ s^{-1}. Inner-shell frequency, ν_{is}, is equal to 5×10^{13} s^{-1} (solid traces) or 5×10^{12} s^{-1} (dashed traces). Upward-going sequence of four traces in each set refer to solvent τ_L^{-1} values of 6×10^{10}, 2×10^{11}, 1×10^{12}, and 6×10^{12} s^{-1} (see refs 64 and 65).

sets of curves shown refer to a quartet of τ_L^{-1} values, varying from 6×10^{10} to 6×10^{12} s^{-1} (the lowest and highest traces, respectively); these values were chosen so to span the commonly encountered dynamical range. The quartet of solid curves refer to an inner-shell (vibrational) frequency, ν_{is}, of 5×10^{13} s^{-1}, whereas the corresponding dashed curves were computed for a 10-fold smaller frequency. The rates were computed chiefly in the manner prescribed by Marcus et al.;[9] full details will be provided elsewhere.[64]

Physically, the dynamical effect of the inner-shell component arises from the provision of additional channels by which the reaction can be consummated once the vicinity of the barrier top is reached. In the absence of such a vibrational reaction coordinate, electron transfer occurs only when the system reaches the barrier cusp entirely by diffusive solvent motion. In the calculations shown in Figure 5, the reaction is considered to be consummated under these latter conditions at the barrier cusp by means of solvent inertial motion (ω_0 is taken to be 10 ps^{-1}); this feature yields a self-consistent kinetic treatment in the absence and presence of the vibrational reaction coordinate.[65]

Examination of Figure 5 reveals several significant features. The inclusion of the inner-shell barrier component initially *increases* the rate constant, even though decreases are seen eventually for moderate ($\gtrsim$0.5–1 kcal mol^{-1}) ΔG^*_{is} values. The former effect is due to the occurrence of an increasingly rapid barrier-crossing frequency, arising from the inclusion of the inner-shell dynamics, offsetting the influences of the larger activation barrier. At a given ν_{is}, the vertical displacement of the various traces shows the sensitivity of the reaction

rate on τ_L^{-1}. As might be expected, this sensitivity decreases progressively as ΔG^*_{is} becomes larger, corresponding to an increasing dominance by the inner-shell dynamics under these conditions. Nevertheless, it is interesting to note that a significant or even substantial dependence of log k_{ex} upon log τ_L^{-1} can remain in the presence of the inner-shell barrier. This is especially the case in the presence of *more rapid* inner-shell dynamics (see the solid versus the dashed traces in Figure 5).

This last property, where the influence of varying solvent friction upon ν_n becomes more pronounced as the overdamped dynamics become *slower*, is in complete contrast to the TST picture. A qualitatively similar prediction can also be deduced[46a] from an earlier theoretical treatment by Ovchinnikova.[66] Moreover, nuclear tunneling can diminish substantially the influence of high-frequency vibrations (say, $\nu_{is} \gtrsim 1 \times 10^{13}$ s^{-1}), enhancing the predicted effects of solvent friction upon k_{ex} even at ambient temperatures.[64] (Nuclear tunneling corrections are not included in Figure 5 for simplicity.) Consequently, then, there are theoretical reasons to anticipate that the barrier-crossing dynamics can be influenced significantly by overdamped solvent motion even in the presence of much more rapid inner-shell barrier components, although the former effects should be largely attenuated when $\Delta G^*_{is} \gtrsim \Delta G^*_{os}$.

Experimental tests of such theoretical predictions for activated ET are so far surprisingly sparse. One contributing factor is that there is a paucity of suitable outer-sphere reactant systems, especially having low charges so to minimize electrostatic work terms, for which the inner-shell barriers are known and preferably are variable by means of suitable chemical modification. One such study for the solvent-dependent electrochemical exchange of cobalt clathrochelates has indicated that significant solvent friction effects can be maintained even when $\Delta G^*_{is} \sim \Delta G^*_{os}$.[57] Some further evidence that the theoretical predictions such as in Figure 5 may overestimate the influence of inner-shell vibrations in muting solvent-friction effects has also been obtained from a recent examination of electrochemical and self-exchange kinetics for various sesquibicyclic hydrazines.[67] One limitation of the theoretical treatment noted above[9] is that it does not consider the effects of barrier-top roundedness arising from electronic coupling. Similar to the discussion in section II, the inevitable presence of this factor is anticipated to enhance the role of solvent friction in mediating the influence of additional vibrational reaction channels upon ν_n.

VII. Activation-Parameter Analyses

As already mentioned, at first sight the evaluation of activation parameters, i.e., temperature-dependent rate measurements, would appear to be a valuable tactic for extracting information on ET barrier-crossing dynamics. At least in principle, the Arrhenius preexponential factor, A_{et}, obtained conventionally from the intercept of ln k_{ex}–T^{-1} plots, should be related closely to the desired frequency factor $\kappa_{el}\nu_n$. The approach has indeed been utilized on a number of occasions with this objective in mind.[38f,43a,46a] Although yielding useful information, at least for bimolecular processes, this procedure suffers from some ambiguities that conspire to render it less useful for assessing $\kappa_{el}\nu_n$.

First, the measured activation enthalpy, and hence the inferred preexponential factor, are expected to be affected by the enthalpic and entropic contributions to the free energy of precursor-complex formation. Such components may well be sensitive to the local solvation and other intermolecular interactions in the precursor state versus the separated reactants to a greater extent than the overall free energy and hence K_p.[68] Even for reactions involving monocharged cation/neutral pairs, such as the metallocene self-exchanges considered above, unexpectedly low Arrhenius preexponential factors, A_{pe}, are obtained that may reflect in part unfavorable entropic contributions to the precursor-complex stability.[43a]

A second complication concerns the anticipated temperature dependence of the barrier-crossing frequency $\kappa_{el}\nu_n$. While the usual Arrhenius treatment tacitly assumes that the overall preexponential factor A_{pe} is temperature independent, this is seldom expected to be the case, especially for barrier crossing controlled by solvent friction. Thus τ_L^{-1}, and hence ν_n, are expected to increase with temperature, thereby yielding inferred A_{pe} values that are larger than $K_p\kappa_{el}\nu_n$.[43a,46a] While this factor can be taken into account in activation-parameter analyses,[43a,46a] such procedures are obliged to rely on the presumed validity of the combined Debye/dielectric continuum or other treatments in accounting for the temperature dependence of the dynamics. Given the likely quantitative limitations of the theoretical treatments noted above, the procedure is susceptible to difficulties so that the resulting preexponential factors tend to provide only an unreliable monitor of ET reaction dynamics.

Nonetheless, under favorable circumstances, such as the examination of rate parameters for related sequences of reactions, the evaluation of activation-parameter data may have considerable virtues for the elucidation of dynamical effects. Indeed, this tactic has been utilized in several solvent dynamical studies, mostly involving small-barrier ET processes.[69] Most importantly, the approach has greatest merit for the examination of intramolecular electron-transfer systems, where the complications associated with the energetics of precursor-complex formation are absent.[70]

VIII. Semiempirical Solvent Analyses

We have so far focused on the interplay between theoretical and experimental aspects of dynamical solvent effects, with a focus on utilizing the former to both describe and elucidate the latter. As in other aspects of electron-transfer chemistry, experimental data has also been used to provide critical tests of specific aspects of the theoretical framework, so that the theory–experiment intercourse has been mutually beneficial. In many facets of experimental chemical kinetics, appeal is usefully made to methods of summarizing and collating the observed trends based on semiempirical solvent and reactant parameters; such approaches have become especially common (and sophisticated) in physical organic chemistry.[71] Not surprisingly, then, several recent studies concerned with

solvent effects in ET kinetics have pursued data analyses using tactics along these lines. We now briefly consider some of these correlation methods, and their possible relation to conventional treatments of ET dynamics.

One simple approach involves correlating solvent-dependent rate data for electron exchange with the macroscopic solvent viscosity, η.[38a,38b,39a,46b,72] The relationship is often found to be satisfactory, especially for electrochemical rate data. This is unsurprising in view of the crude correlation observed (and predicted[73]) between η and τ_D (and hence with τ_L via eq 10), at least for adiabatic reactions where the outer-shell barrier does not vary greatly so that roughly $k_{ex} \propto \nu_n$. The observation of such k_{ex}–η^{-1} relationships, however, may also portend the presence of artifacts in the rate data arising from reactant diffusion and/or solution resistance (vide supra), since the latter parameters correlate closely with solvent viscosity. One oft-cited study found such correlations for rate constants for electrochemical exchange of $Fe(CN)_6^{3-/4-}$ and $Cp_2Fe^{+/0}$ with viscosity increases in water and dimethyl sulfoxide, respectively, caused by the addition of sugars.[72] These findings are, however, difficult (and ambiguous) to interpret in a microscopic sense; in any case, such a relationship was not observed in related measurements for a homogeneous self-exchange reaction.[38b]

Not surprisingly, multiparametric methods utilizing specific solvent properties can describe the solvent dependence of ET rates in a number of cases. One recent example[74] employs solvent acidity, basicity, and polarizability parameters according to the Taft et al. treatment[75] to achieve correlations with solvent-dependent k_{ex} data that are touted to be superior to those obtained by using the conventional dielectric-continuum model. The version of the latter used in ref 74, however, did not consider solvent dynamics (it was essentially method I described in section III). The physical significance of the findings are therefore questionable at best. More generally, it is worth noting that improved "fits" to experimental data achieved by multiparametric analyses can often be the inevitable result of the additional variables employed rather than signaling a physically meaningful finding!

As a final example, Nelsen et al. have related solvent-dependent self-exchange rates for a sesquibicyclic hydrazine with the Kosower Z parameter.[76] They note that better correlations are achieved than by using the conventional dielectric continuum model, either with or without consideration of solvent dynamics. In the latter case, a reasonable correspondence is actually obtained, except the rates obtained in alcohol solvents are anomously low. The reasons for such deviations are unclear at present; it would clearly be desirable to obtain optical ET energies for mixed-valence hydrazine analogues so to check the applicability of eq 12 or related continuum treatments of the outer-shell barrier. Indeed, such optical data are conspicuous by their absence for organic radical redox systems.

Overall, then, while semiempirical solvent analyses retain a place in the armory of chemists seeking to rationalize solvent effects in ET reactions, a greater emphasis should perhaps be placed in relating these approaches to the inherently more fundamental theoretical treatments now available for describing the dynamics as well as energetics of such processes.

IX. Some Problems and Unresolved Issues: When Do Solvent-Friction Effects Matter?

In some respects, our current understanding of dynamical solvent effects in activated ET processes might be deemed satisfactory. While many quantitative (and important) details are lacking, there is widespread evidence available from solvent-dependent electron-exchange studies of the importance of overdamped solvent relaxation to the reaction dynamics. An initial quantitative link has been made with the real-time dynamical information obtainable from TDFS measurements, and the rough applicability of continuum–Debye descriptions of solvent dynamics established, along with the likely importance of rapid overdamped components, in some cases. The central role of donor–acceptor electronic coupling in mediating the occurrence, as well as the characteristics, of such nuclear dynamical effects has also become apparent on an experimental as well as a theoretical basis.

There are some reasons, however, to suspect that this scenario may be overly optimistic or perhaps even misleading. First, our understanding of the type and range of activated ET processes susceptible to dynamical solvent effects is discomfortingly inadequate. This situation is related to a lack of reliable independent information on electronic coupling, especially for electrochemical reactions. The extent of solvent dynamical effects often observed for such processes[38,39] infer that substantial electronic coupling, $H_{12} \gtrsim 0.5$ kcal mol^{-1}, is commonly present. While there is some theoretical justification for the presence of such electronic coupling for reactions at metal surfaces,[77] the broad-based occurrence of adiabatic pathways for outer-sphere reactions, as inferred from the rate-solvent behavior, would be surprising.

Unfortunately, a large fraction of the electrochemical reactions amenable to such solvent-dependent analysis exhibit k_{ex} values (ca. 0.1–10 cm s^{-1}) that approach (or even surpass?) the limit that can be evaluated reliably even by contemporary kinetic techniques, such as ac impedance and/or microelectrode-based approaches. As mentioned above, this problem can be particularly insidious since the resulting systematic errors in the rate data have a solvent-dependent character which is similar to that expected in the presence of solvent dynamical effects. Given the additional uncertainties associated with the usage of dielectric-continuum estimates of ΔG^*_{os} to electrochemical systems, there are good reasons to be wary of some dynamical analyses undertaken for electrochemical systems. Related difficulties can also hamper analyses for some homogeneous-phase reactions. For example, very rapid self-exchange reactions, having rates approaching the bimolecular diffusion limit, can yield solvent-dependent rate behavior reminiscent of dynamical solvent relaxation merely as a result of viscosity-dependent solute transport effects.

Another significant unresolved issue, again associated with electronic-coupling effects, concerns the likely importance of solvent relaxation within the reactant (and product) free-energy wells versus that in the barrier-top region. For cusp barriers, featured in the original Zusman model[6] (leading to eq 9) as well as numerous subsequent theoretical treatments, the former component is necessarily dominant. However, this dynamical model is inherently somewhat artificial since cusp

barriers arise from the circumstance $H_{12} \rightarrow 0$, where electron tunneling rather than nuclear dynamics will actually control the net barrier-crossing frequency. Recent MD simulations performed for a "model aprotic" solvent with a reaction involving moderate or large electronic coupling (H_{12} = 1 and 5 kcal mol^{-1}, respectively) yielded little evidence of any solvent friction in the former case and mild friction arising from overdamped motion only within the barrier-top region in the latter circumstance.[17,78] The solvent model employed in these studies appears to exhibit only low-friction characteristics. Nevertheless, it is disquieting to note that there is apparently no evidence so far from MD simulations for the occurrence of ET solvent friction associated with well relaxation, the observed rate diminutions being associated only with recrossings within the barrier-top region.[17,78]

As already noted, there is good reason to expect overdamped motion in the barrier-top versus the well regions to become a more prevalent contributor to ν_n as the electronic coupling increases, and hence the effective "barrier-top frequency", ω_b, decreases to the extent that it becomes comparable to the well frequency, ω_0.[8c,30] Given the general requirement that at least moderate electronic coupling be present to engender nuclear-dynamical control, it is conceivable that the solvent friction observed experimentally for activated ET processes arises chiefly from relaxation within the barrier-top region. This circumstance would of course be aided by reaction pathways that utilize preferentially reaction geometries having especially large electronic couplings. Such a circumstance is plausible: for example, for $Cp_2Co^{+/0}$ self-exchange where one specific (D_{5h}) internuclear geometry is predicted to yield especially strong coupling, $H_{12} \simeq 2.5$ kcal mol^{-1}.[47a,79] Further MD simulations, however, preferably for realistic overdamped model solvents, are required to resolve this critical question.

X. Future Directions

On the basis of the foregoing, progress in our experimental elucidation of solvent dynamics in ET reactions, as perhaps for other condensed-phase chemical processes, would appear to stand at the crossroads. The separation between energetic and dynamical factors, required for exposure of the latter in all activated processes, has been achieved with some confidence for some outer-sphere ET reactions, but usually by resorting to the use of theoretical estimates of the solvent-dependent barrier height. A number of organometallic and organic redox couples have been examined in a variety of largely ambient temperature solvents. While judicious choices of solvents and especially reactant systems have often been made for the purpose at hand, the validity of the data analyses often appears to be questionable. This difficulty has been exacerbated by a significant lack of appreciation of the likely limitations of the dielectric-continuum models usually employed for such analyses. That is not to say that such studies should be discouraged—much has been learned already from the experimental examination of solvent effects in electron-exchange reactions—however, the dissection of energetic and dynamical factors in rate data remains a key stumbling block to true progress in our understanding of ET solvent dynamics. As a consequence, there remains a substantial gulf between the levels of sophistication of the theoretical predictions and experimental interrogation—a situation that also applies more generally to electron-transfer chemistry.

It appears that this difficulty could be diminished by devoting greater attention in the future to the experimental evaluation of electron-transfer barriers by optical measurements. A general limitation of experimental studies so far, however, is that the range of ET reaction types explored is relatively narrow, being restricted almost entirely to outer-sphere electron-exchange processes. It would be desirable, for example, to examine exoergic processes, such as homogeneous-phase cross reactions, in this context. Similar analyses could be undertaken as outlined above, although it is necessary to correct the observed solvent-dependent rates for variations in the thermodynamic driving-force contribution to ΔG^* present for cross reactions. At least one study along these lines has recently been reported.[82] Especially given the central influence of electronic coupling in the reaction dynamics, it would be of particular interest to examine inner-sphere ET and other "strong-overlap" charge-transfer reactions. Despite the extensive theoretical and computational work on some aspects of strong-overlap charge-transfer processes,[83] related solvent-dependent experimental studies are rare. An interesting recent example, however, concerns the evaluation of primary kinetic isotope effects (k_H/k_D) for hydride transfer.[84] A significant solvent dependence of k_H/k_D was observed, from a maximum of ca. 5–5.5 in low-friction media to ca. 3.0 in some other solvents. Although a quantitative relationship between k_H/k_D and solvent friction was not established, the results are roughly consistent with a shift from near-complete rate control by hydride tunneling to partial control by overdamped solvent dynamics.[84] This interpretation is closely analogous to the phenomenon of solvent-friction-dependent adiabaticity for electron transfer, embodied in Figures 3 and 4.

Most importantly, it would be very desirable to explore the kinetics of unimolecular, preferably rigid intramolecular, ET processes with regard to solvent dynamical effects. Compared with bimolecular (and electrochemical) processes, such systems have the major virtue of eliminating uncertainties regarding the energetics and geometries of precursor-complex formation. Although a number of photoexcited intramolecular ET reactions have been examined,[18] as mentioned above, these apparently feature small or negligible ($\lesssim k_BT$) barriers; few such studies involving *activated* intramolecular ET process have been reported so far. Although experimental difficulties need to be overcome, there are good reasons to emphasize intramolecular ET processes in future studies. It will be desirable to identify reactant systems for which *both* optical ET energetics and thermal ET rates can be obtained, thereby enabling reliable separations between dynamical and energetic factors to be achieved. The evaluation of activation parameters should also prove to be valuable in this regard, the complications of the precursor-formation energetics that plague their interpretation for intermolecular systems being absent.

Such unimolecular systems should also be useful for expanding experimental inquiries of dynamical effects into a wider range of solvating environments, such as polymers[82] and glasses. Another novel variant of a

electron-transfer system for which unimolecular rates can be extracted involves films of redox-active species at solvent–air interfaces, along which redox-mediated electron transport can be evaluated.[85] Interestingly, there is evidence that solvent dynamics can limit electron transfer in such systems, as deduced from the dependence of the transport rates through Os(III)/(II) tris(diphenylphenanthrolene) films upon the nature of the solvent molecules accumulated at the nominal water–air interface.[85b]

Overall, then, there is some reason to be optimistic that our understanding of solvent-friction, as for other dynamical, aspects of ET reaction kinetics can be placed on an increasingly diverse as well as firm experimental basis in the future. Such studies, especially in conjunction with other information, such as that obtained from MD simulations and electronic structural calculations, should lead to a deeper understanding of some of these fascinating mysteries surrounding solvent and related environmental effects in charge-transfer processes.

Glossary of Terms

ΔG^*_{os}	outer-shell (solvent reorganization) barrier
ΔG^*_{is}	inner-shell (reactant intramolecular) barrier
ϵ_{op}	solvent optical dielectric constant
ϵ_∞	"infinite-frequency" (ca. microwave frequency) dielectric constant
ϵ_0	solvent static (zero frequency) dielectric constant
κ_{el}	electronic transmission coefficient
H_{12}	electronic matrix coupling element
ν_n	nuclear frequency factor
K_p	equilibrium constant for forming precursor state for bimolecular (or electrochemical) reaction
k_{et}	rate constant for (unimolecular) reaction within precursor state
k_{ex}	rate constant for overall homogeneous self-exchange, or electrochemical exchange, reaction
τ_L	longitudinal solvent relaxation time
τ_D	Debye solvent relaxation time

Aknowledgments

The continued financial support of our research on this topic by the Office of Naval Research is gratefully acknowledged. I am thankful for the industrious efforts of my co-workers in this area since 1984—Roger Nielson, Alex Gochev, Neal Golovin, Tom Gennett, Don Phelps, and especially the late George McManis. I remain indebted to George, in particular, for sharing with me a wondrous sense of excitement (and sheer fun), as well as fulfillment, in exploring this enticing area of physical chemistry.

References and Notes

(1) (a) Marcus, R. A. *J. Chem. Phys.* **1956**, *24*, 966; 979. (b) Marcus, R. A. *J. Chem. Phys.* **1965**, *43*, 679. (c) Marcus, R. A. *Ann. Rev. Phys. Chem.* **1964**, *15*, 155.
(2) For overviews of electron-transfer models within the framework of the TST treatment, see: (a) Sutin, N. *Acc. Chem. Res.* **1982**, *15*, 275. (b) Sutin, N. *Prog. Inorg. Chem.* **1983**, *30*, 441.
(3) Explanative broad-based reviews include: (a) Hynes, J. T. In *The Theory of Chemical Reactions*; Baer, M., Ed.; CRC Press: Boca Raton, FL, 1985; Vol. 4, p 171. (b) Hynes, J. T. *J. Stat. Phys.* **1986**, *42*, 149. (c) Chandler, D. *J. Stat. Phys.* **1986**, *42*, 49.
(4) McManis, G. E.; Gochev, A.; Weaver, M. J. *Chem. Phys.* **1991**, *152*, 107, and references cited therein.
(5) Kramers, H. A. *Physica* **1940**, *7*, 284.
(6) Zusman, L. D. *Chem. Phys.* **1980**, *49*, 295.
(7) (a) Calef, D. F.; Wolynes, P. G. *J. Phys. Chem.* **1983**, *87*, 3387. (b) Wolynes, P. G. *J. Chem. Phys.* **1987**, *86*, 5133.
(8) (a) van der Zwan, G.; Hynes, J. T. *J. Chem. Phys.* **1982**, *76*, 2993. (b) van der Zwan, G.; Hynes, J. T. *Chem. Phys. Lett.* **1983**, *101*, 367. (c) Hynes, J. T. *J. Phys. Chem.* **1986**, *90*, 3701. (d) van der Zwan, G.; Hynes, J. T. *Chem. Phys.* **1991**, *152*, 169.
(9) (a) Sumi, H.; Marcus, R. A. *J. Chem. Phys.* **1986**, *84*, 4894. (b) Nadler, W.; Marcus, R. A. *J. Chem. Phys.* **1987**, *86*, 3906.
(10) (a) Rips, I.; Jortner, J. *J. Chem. Phys.* **1987**, *87*, 2090. (b) Rips, I.; Klafter, J.; Jortner, J. *J. Chem. Phys.* **1988**, *89*, 4288.
(11) Belousov, A. A.; Kuznetsov, A. M.; Ulstrup, J. *Chem. Phys.* **1989**, *129*, 311.
(12) Newton, M. D.; Friedman, H. L. *J. Chem. Phys.* **1988**, *88*, 4460.
(13) (a) Morillo, M.; Cukier, R. I. *J. Chem. Phys.* **1988**, *89*, 6736. (b) Yang, D. Y.; Cukier, R. I. *J. Chem. Phys.* **1989**, *91*, 281.
(14) (a) Sparpaglione, M.; Mukamel, S. *J. Phys. Chem.* **1987**, *91*, 3938. (b) Sparpaglione, M.; Mukamel, S. *J. Chem. Phys.* **1988**, *88*, 1465. (c) Yau, Y. J.; Sparpaglione, M.; Mukamel, S. *J. Phys. Chem.* **1988**, *92*, 4842.
(15) (a) Bagchi, B.; Chandra, A.; Fleming, G. R. *J. Phys. Chem.* **1990**, *94*, 5197. (b) Chandra, A.; Bagchi, B. *J. Phys. Chem.* **1989**, *93*, 6996.
(16) For reviews of analytic theory, see: (a) Onuchic, J. N.; Wolynes, P. G. *J. Phys. Chem.* **1988**, *92*, 6495. (b) Bagchi, B. *Ann. Rev. Phys. Chem.* **1989**, *40*, 115. (c) Kuznetsov, A. M.; Ulstrup, J.; Vorotyntsev, M. A. In *Chemical Physics of Solvation*; Dogonadze, R. R., Kalman, E., Kornyshev, A. A., Ulstrup, J., Eds.; Elsevier: Amsterdam, 1988; Part C, Chapter 3. (d) Mukamel, S.; Yan, Y. T. *Acc. Chem. Res.* **1989**, *22*, 301.
(17) (a) Zichi, D. A.; Ciccotti, G.; Hynes, J. T.; Ferrario, M. *J. Phys. Chem.* **1989**, *93*, 6261. (b) Bader, J. S.; Kuharski, R. A.; Chandler, D. *J. Chem. Phys.* **1990**, *93*, 230.
(18) For overviews, see: (a) Barbara, P. F.; Jarzeba, W. *Adv. Photochem.* **1990**, *15*, 1. (b) Bagchi, B.; Fleming, G. R. *J. Phys. Chem.* **1990**, *94*, 9. (c) Simon, J. D. *Pure Appl. Chem.* **1990**, *62*, 2243.
(19) For overviews see: (a) Maroncelli, M. *J. Mol. Liq.*, in press. (b) Maroncelli, M.; MacInnis, J.; Fleming, G. R. *Science* **1989**, *243*, 1674. (c) Simon, J. D. *Acc. Chem. Res.* **1988**, *21*, 128.
(20) Weaver, M. J.; McManis, G. E. *Acc. Chem. Res.* **1990**, *23*, 294.
(21) Brown, G. M.; Sutin, N. *J. Am. Chem. Soc.* **1979**, *101*, 883.
(22) Hupp, J. T.; Weaver, M. J. *J. Electroanal. Chem.* **1983**, *152*, 1.
(23) The units of K_p, M^{-1} and cm, for homogeneous and electrochemical reactions, respectively, account for the usual k_{ob} units, M^{-1} s^{-1} and cm s^{-1}, given that k_{et} is a unimolecular rate constant for reaction within a given precursor geometry.
(24) (a) Tembe, B. L.; Friedman, H. L.; Newton, M. D. *J. Chem. Phys.* **1982**, *76*, 1490. (b) Newton, M. D.; Sutin, N. *Annu. Rev. Phys. Chem.* **1984**, *35*, 437.
(25) Gochev, A.; McManis, G. E.; Weaver, M. J. *J. Chem. Phys.* **1989**, *91*, 906.
(26) Note that the oft-quoted eq 9 is a special case of relationships given in refs 6 and 7a (and elsewhere) when $\Delta G° = 0$.
(27) For reviews of the interpretation of dielectric loss spectra, see: (a) Hill, N. E.; Vaughan, W. E.; Price, A. H.; Davis, M. *Dielectric Properties and Molecular Behavior*; Van Nostrand Reinhold: London, 1969. (b) Böttcher, C. J. F.; Bordewijk, P. *Theory of Electric Polarization*; Elsevier: Amsterdam, 1978.
(28) For an erudite discussion of the meaning of τ_L in relation to τ_D, see: Kivelson, D.; Friedman, H. *J. Phys. Chem.* **1989**, *93*, 7026.
(29) McManis, G. E.; Nielson, R. M.; Gochev, A.; Weaver, M. J. *J. Am. Chem. Soc.* **1989**, *111*, 5533.
(30) McManis, G. E.; Weaver, M. J. *J. Chem. Phys.* **1989**, *90*, 912.
(31) For example, see: (a) Garg, S. K.; Symth, C. P. *J. Phys. Chem.* **1965**, *69*, 1294. (b) Crossley, J. *Adv. Mol. Relax. Processes* **1970**, *2*, 69.
(32) Onsager, L. *Can. J. Chem.* **1977**, *55*, 1819.
(33) (a) Maroncelli, M.; Fleming, G. R. *J. Chem. Phys.* **1987**, *86*, 6221. But see erratum in *J. Chem Phys.* **1990**, *92*, 3251. (b) Maroncelli, M.; Fleming, G. R. *J. Chem. Phys.* **1988**, *89*, 875.
(34) (a) Kahlow, M. A.; Jarzeba, W. T.; Kang, T. J.; Barbara, P. F. *J. Chem. Phys.* **1989**, *90*, 151. (b) Jarzeba, W.; Walker, G. C.; Johnson, A. E.; Barbara, P. F. *Chem. Phys.* **1991**, *152*, 57.
(35) (a) Chandra, A.; Bagchi, B. *J. Chem. Phys.* **1989**, *90*, 7338. (b) Chandra, A.; Bagchi, B. *J. Phys. Chem.* **1989**, *93*, 6996.
(36) Kornyshev, A. A.; Kuznetsov, A. M.; Phelps, D. K.; Weaver, M. J. *J. Chem. Phys.* **1989**, *91*, 7159.
(37) McManis, G. E.; Mishra, A. K.; Weaver, M. J. *J. Chem. Phys.* **1987**, *86*, 5550.

(38) (a) Harrer, W.; Grampp, G.; Jaenicke, W. *Chem. Phys. Lett.* **1984**, *112*, 263. (b) Harrer, W.; Grampp, G.; Jaenicke, W. *J. Electroanal. Chem.* **1986**, *209*, 223. (c) Kapturkiewicz, A.; Jaenicke, W. *J. Chem. Soc., Faraday Trans. 1* **1987**, *83*, 2727. (d) Grampp, G.; Harrer, W.; Jaenicke, J. *Chem. Soc., Faraday Trans. 1* **1987**, *83*, 161. (e) Grampp, G.; Harrer, W.; Jaenicke, W. *J. Chem. Soc., Faraday Trans. 1* **1988**, *84*, 366. (f) Grampp, G.; Kapturkiewicz, A.; Jaenicke, W. *Ber. Bunseng. Phys. Chem.* **1990**, *94*, 439. (g) Grampp, G.; Harrer, W.; Hetz, G. *Ber. Bunsenges. Phys. Chem.* **1990**, *94*, 1343. (h) Grampp, G.; Jaenicke, W. *Ber. Bunsenges. Phys. Chem.* **1991**, *95*, 904.

(39) (a) Kapturkiewicz, A.; Behr, B. *J. Electroanal. Chem.* **1984**, *179*, 187. (b) Kapturkiewicz, A.; Opallo, M. *J. Electroanal. Chem.* **1985**, *185*, 15. (c) Kapturkiewicz, A. *Electrochim. Acta* **1985**, *30*, 1301. (d) Opallo, M. *J. Chem. Soc., Faraday Trans. 1* **1986**, *82*, 339.

(40) (a) Dzhavakhidze, P. G.; Kornyshev, A. A.; Krishtalik, L. I. *J. Electroanal. Chem.* **1987**, *228*, 329. (b) Phelps, D. K.; Kornyshev, A. A.; Weaver, M. J. *J. Phys. Chem.* **1990**, *94*, 1454.

(41) For an explanative review, see: Creutz, C. *Prog. Inorg. Chem.* **1983**, *30*, 1.

(42) Nielson, R. M.; Golovin, M. N.; McManis, G. E.; Weaver, M. J. *J. Am. Chem. Soc.* **1988**, *110*, 1745.

(43) (a) Neilson, R. M.; McManis, G. E.; Golovin, M. N.; Weaver, M. J. *J. Phys. Chem.* **1988**, *92*, 3441. (b) Nielson, R. M.; McManis, G. E.; Safford, L. K.; Weaver, M. J. *J. Phys. Chem.* **1989**, *93*, 2152. (c) Nielson, R. M.; McManis, G. E.; Weaver, M. J. *J. Phys. Chem.* **1989**, *93*, 4703.

(44) McManis, G. E.; Gochev, A.; Nielson, R. M.; Weaver, M. J. *J. Phys. Chem.* **1989**, *93*, 7733.

(45) (a) Note that the solvent-dependent rate constants for $Cp_2Fe^{+/0}$ self-exchange listed in Table I, taken from refs 29 and 43b, differ significantly from earlier published values;[45b] as discussed in ref 43b the latter values suffer from systematic errors in the NMR line-broadening analysis. (b) Yang, E. S.; Chan, M.-S.; Wahl, A. C. *J. Phys. Chem.* **1980**, *84*, 3094.

(46) (a) Gennett, T.; Milner, D. F.; Weaver, M. J. *J. Phys. Chem.* **1985**, *89*, 2787. (b) McManis, G. E.; Golovin, M. N.; Weaver, M. J. *J. Phys. Chem.* **1986**, *90*, 6563.

(47) (a) Newton, M. D.; Ohta, K.; Zhang, E. *J. Phys. Chem.* **1991**, *95*, 2317. (b) Also see: Newton, M. D. *Chem. Rev.* **1991**, *91*, 767.

(48) Phelps, D. K.; Gord, J. R.; Freiser, B. S.; Weaver, M. J. *J. Phys. Chem.* **1991**, *95*, 4338.

(49) The recognition that κ_{el}, and hence $\kappa_{el}K_p$, will depend inherently on ν_n for weakly adiabatic as well as nonadiabatic processes has not always been made in the recent literature (for example, see ref 50).

(50) Fawcett, W. R.; Foss, C. A. *J. Electroanal. Chem.* **1988**, *252*, 221.

(51) Chan, M.-S.; Wahl, A. C. *J. Phys. Chem.* **1982**, *86*, 126.

(52) Weaver, M. J.; Phelps, D. K.; Nielson, R. M.; Golovin, M. N.; McManis, G. E. *J. Phys. Chem.* **1990**, *94*, 2949.

(53) For example: (a) Brandon, J. R.; Dorfman, L. M. *J. Chem. Phys.* **1970**, *53*, 3849. (b) Li, T. T.-T.; Brubaker, C. H., Jr. *J. Organomet. Chem.* **1981**, *216*, 223.

(54) An examination of these effects utilizing optical electron-transfer energies is described: (a) Blackburn, R. L.; Hupp, J. T. *Chem. Phys. Lett.* **1988**, *150*, 399. (b) Blackburn, R. L.; Hupp, J. T. *J. Phys. Chem.* **1990**, *94*, 1788. A discussion of the physical concepts embodied in the form of eqs 12 and 13, and their applicability, are given: (c) Hupp, J. T.; Weaver, M. J. *J. Phys. Chem.* **1985**, *89*, 1601.

(55) (a) Beretan, D. N.; Onuchic, J. N. *J. Chem. Phys.* **1988**, *89*, 6195. (b) Onuchic, J. N.; Beretan, D. N. *J. Phys. Chem.* **1988**, *92*, 4818.

(56) For example: Fawcett, W. R.; Foss, C. *J. Electroanal. Chem.* **1989**, *270*, 103.

(57) Nielson, R. M.; Weaver, M. J. *J. Electroanal. Chem.* **1989**, *260*, 15.

(58) Nielson, R. M.; Weaver, M. J. *Organometallics* **1989**, *8*, 1636.

(59) Also consistent with this notion, Wherland et al.[60] have observed a k_{ex} value for $Cp_2Ni^{+/0}$ in dichloromethane which is even faster than for $Cp_2Co^{+/0}$; the former couple contains two electrons in the ligand-centered HOMO $4e_{ig}^*$ orbital versus one electron for the latter redox system.

(60) Gribble, J. D.; Wherland, S. *Inorg. Chem.* **1990**, *29*, 1130.

(61) Weaver, M. J.; McManis, G. E.; Jarzeba, W.; Barbara, P. F. *J. Phys. Chem.* **1990**, *94*, 1715.

(62) Zusman, L. D. *Chem. Phys.* **1988**, *119*, 51.

(63) (a) Fonseca, T. *Chem. Phys. Lett.* **1989**, *162*, 491. (b) Fonseca, T. *J. Chem. Phys.* **1989**, *91*, 2869.

(64) The rate constant k_{ex} is obtained from the inverse "average first-passage survival time" τ_s^{-1}, employed in ref 9.[55]

(65) Phelps, D.; Weaver, M. J. *J. Phys. Chem.*, submitted for publication.

(66) Ovchinnikova, M. Ya *Russ. Theoret. Exp. Chem.* **1981**, *17*, 507.

(67) Phelps, D.; Nelsen, S. F.; Weaver, M. J. In preparation.

(68) For a recent theoretical study, see: Morita, T.; Ladanyi, B. M.; Hynes, J. T. *J. Phys. Chem.* **1989**, *93*, 1386.

(69) (a) McGuire, M.; McLendon, G. *J. Phys. Chem.* **1986**, *90*, 2547. (b) Vanthey, E.; Suppan, P. *Chem. Phys.* **1989**, *139*, 381. (c) Heitele, H.; Michel-Beyerle, M. E.; Finckh, P. *Chem. Phys. Lett.* **1987**, *138*, 237. (d) Harrison, R. J.; Pearce, B.; Beddard, G. S.; Cowan, J. A.; Sanders, J. K. M. *Chem. Phys.* **1987**, *116*, 429.

(70) For example, see: (a) Haim, A. *Prog. Inorg. Chem.* **1983**, *30*, 273. (b) Isied, S. S. *Prog. Inorg. Chem.* **1984**, *32*, 443.

(71) For example, see: Reichardt, C. *Solvent Effects in Organic Chemistry*; Verlag Chemie: New York, 1979.

(72) Zhang, X.; Leddy, J.; Bard, A. J. *J. Am. Chem. Soc.* **1985**, *107*, 3719.

(73) Davies, M. In ref 27a, Chapter 5.

(74) Abbott, A. P.; Rusling, J. F. *J. Phys. Chem.* **1990**, *94*, 8910.

(75) For example: (a) Kamlet, M. J.; Abboud, J. L. M.; Abraham, M. H.; Taft, R. W. *J. Org. Chem.* **1983**, *48*, 2877. (b) Kamlet, M. J.; Abboud, J. L. M.; Taft, R. W. *Prog. Phys. Org. Chem.* **1981**, *13*, 485.

(76) Nelsen, S. F.; Kim, Y.; Blackstock, S. C. *J. Am. Chem. Soc.* **1989**, *111*, 2045.

(77) (a) Morgan, T. D.; Wolynes, P. G. *J. Phys. Chem.* **1987**, *91*, 874. (b) Zusman, L. D. *Chem. Phys.* **1987**, *112*, 53.

(78) (a) Hynes, J. T.; Carter, E. A.; Cicotti, G.; Kim, H. J.; Zichi, D. A.; Ferrario, M.; Kapral, R. In *Perspectives in Photosynthesis*; Jortner, J., Pullman, B., Eds.; Kluwer Pub.: Dordrecht, 1990; p 133. (b) Smith, B. B.; Kim, H. J.; Hynes, J. T. In *Condensed Matter Physics Aspects of Electrochemistry*; Tosi, M. P., Kornyshev, A. A., Eds.; World Scientific Pub.: Singapore, in press.

(79) Also of relevance to this issue is the recent theoretical treatment of Kim and Hynes that predicts that the effect of H_{12} in diminishing the barrier height ΔG^* is considerably less than the usually applied formula $\Delta G^* = \Delta G_0^* - H_{12}$, where ΔG_c^* is the cusp barrier height.[78,80] The modification arises from a treatment of the coupling between the electronic polarization and the reactant charge distribution. The corresponding effects on the reaction *dynamics*, however, appear to be small.[80] In addition, a critical limitation of this treatment has recently become apparent.[81]

(80) (a) Kim, H. J.; Hynes, J. T. *J. Phys. Chem.* **1990**, *94*, 2736. (b) Kim, H. J.; Hynes, J. T. *J. Chem. Phys.* **1990**, *93*, 5194; 5211.

(81) (a) Gehlen, J. N.; Chandler, D.; Kim, H. J.; Hynes, J. T. *J. Phys. Chem.*, in press. (b) Kim, H. J.; Hynes, J. T. *J. Chem. Phys.*, in press.

(82) Zhang, H.; Murray, R. W. *J. Am. Chem. Soc.* **1991**, *113*, 5183.

(83) For example: Gertner, B. J.; Wilson, K. R.; Hynes, J. T. *J. Chem. Phys.* **1989**, *90*, 3537.

(84) Kreevoy, M. M.; Kotchevar, A. T. *J. Am. Chem. Soc.* **1990**, *112*, 3579.

(85) (a) Charych, D. H.; Landau, E. M.; Majda, M. *J. Am. Chem. Soc.* **1991**, *113*, 3340. (b) Majda, M. Personal communication, December 1991.